Propagation mode and sources location of the Jovian narrowband radiations from 3D numerical modeling of Juno/Waves observations

Adam BOUDOUMA - PRE X 2025, Marseille

INSTITUTE OF ATMOSPHERIC PHYSICS
CAS

LIRA Observatoire de Paris | PSL

The jovian radio emissions

- QP : quasi-periodic burst
- bKOM : broadband kilometric
- HOM : hectometric
- DAM : decametric
- Io-DAM : decametric induced by Io
- Ga-DAM : decametric induced by Ganymede
- Etc…

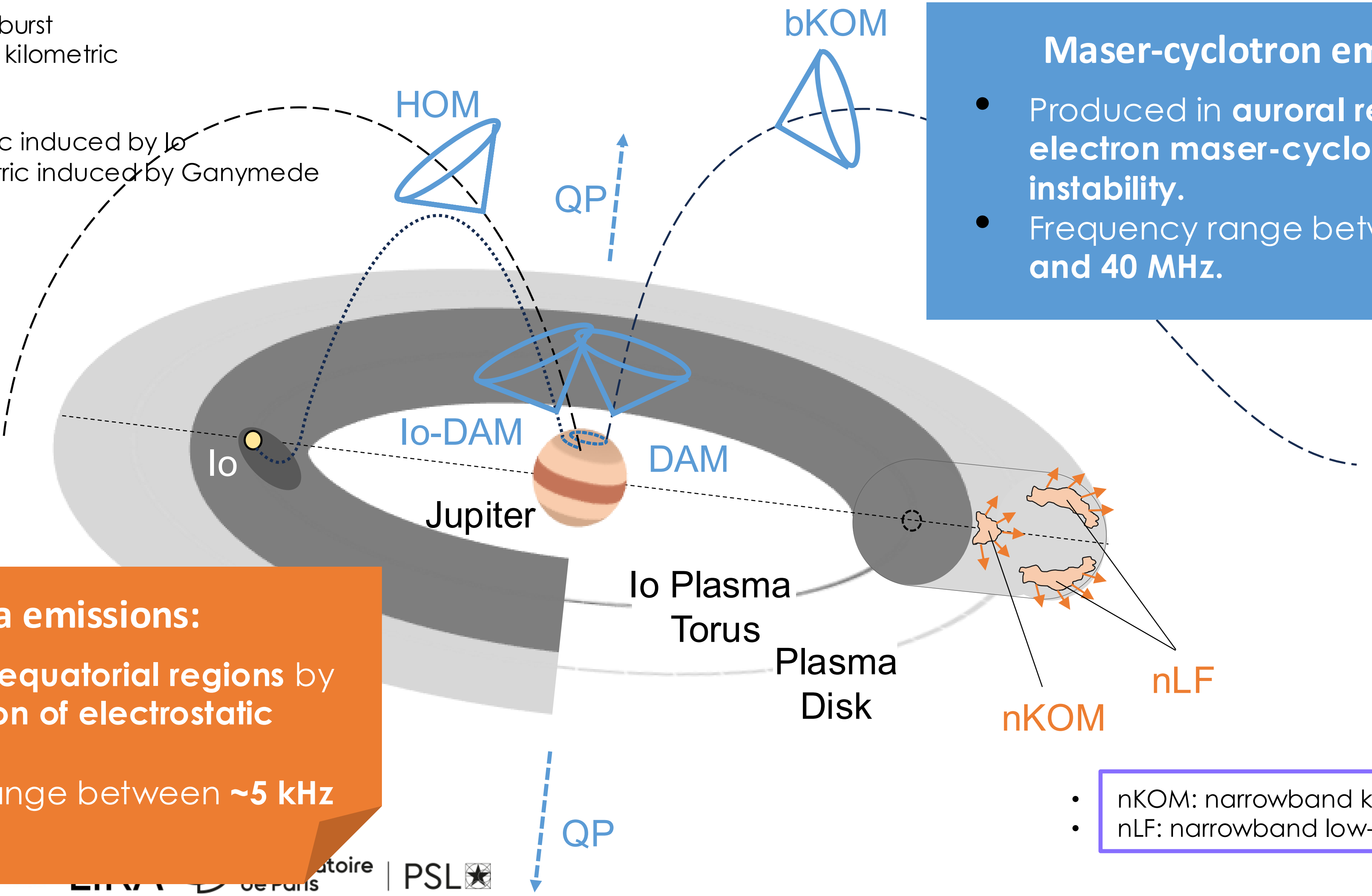

Maser-cyclotron emissions :

- Produced in **auroral regions** by the **electron maser-cyclotron instability.**
- Frequency range between **1 kHz and 40 MHz.**

Plasma emissions:

- Produced in **equatorial regions** by the **conversion of electrostatic waves.**
- Frequency range between **~5 kHz and 200 kHz.**

- nKOM: narrowband kilometric
- nLF: narrowband low-frequency

The Juno mission

- Juno mission (2016 – 2025?):
  - **Polar orbits** with **close flybys of the poles (<10000 km).**
  - **Massive observational data base** (currently 9 years).
  - ***In-situ* measurements** in the plasma disk since ~2023.

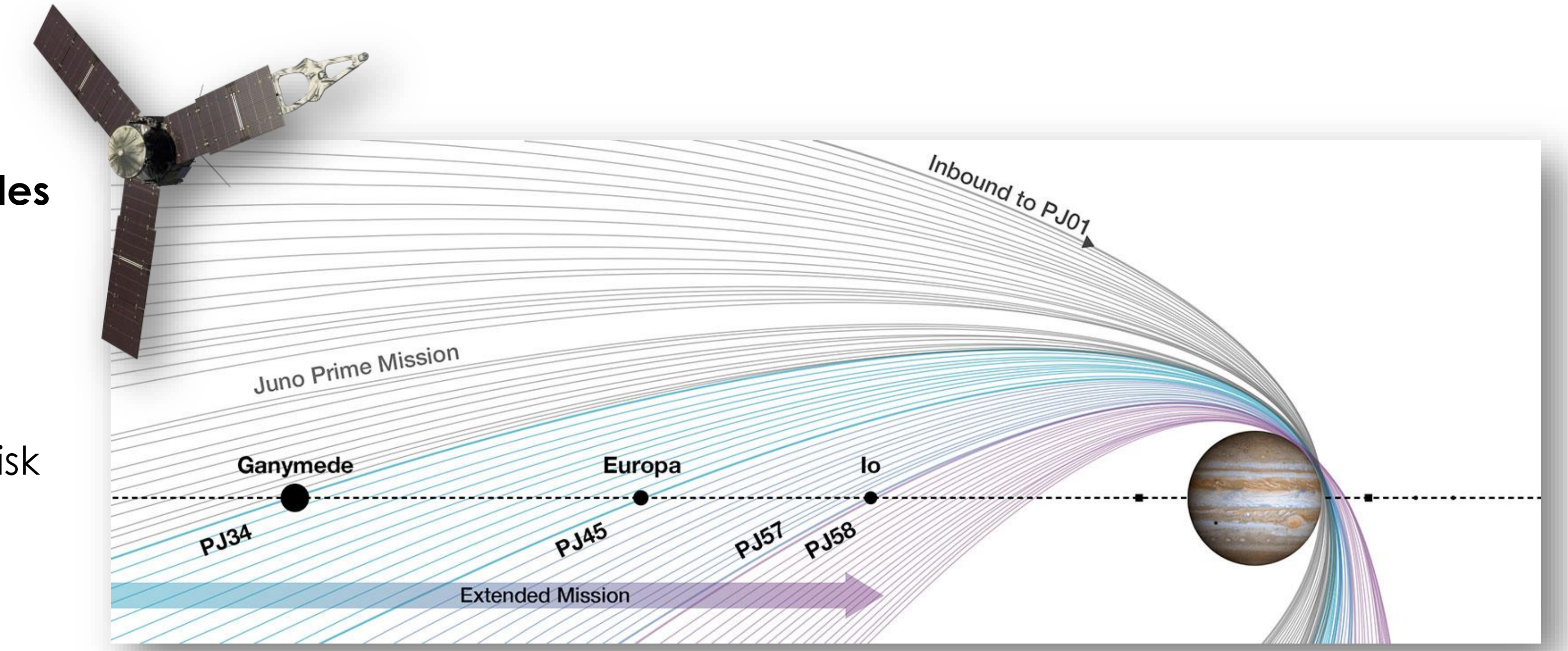

Trajectory of the Juno probe for the initial period 2016-2021 (prime mission) and extended >2021 (extended mission)

Radio observations with the Waves instrument

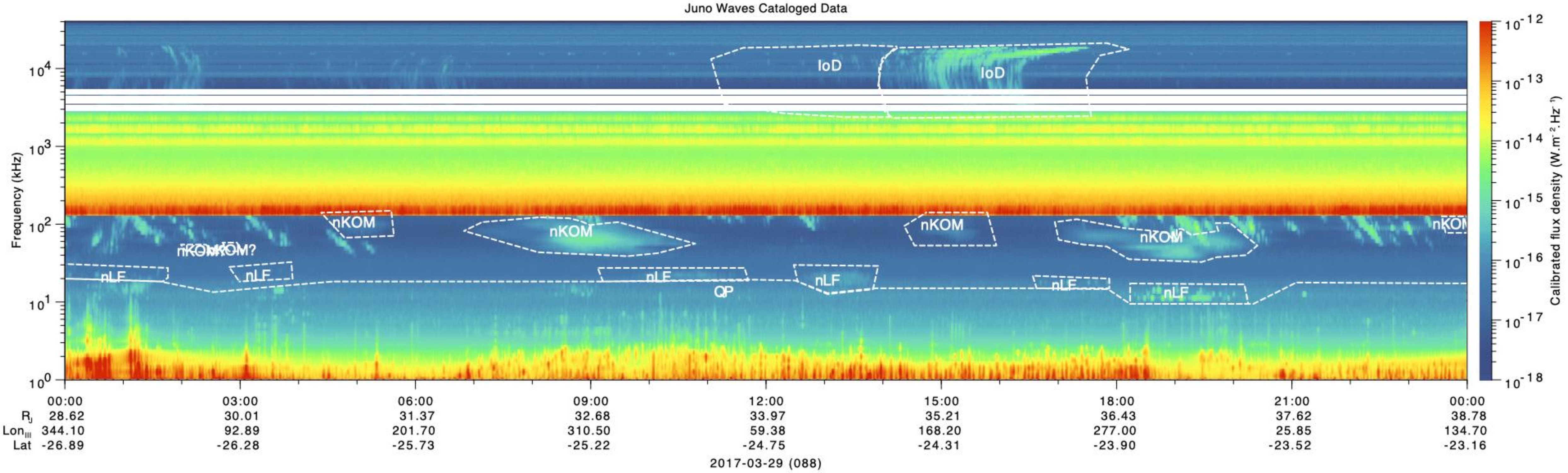

Time-frequency spectrogram of Juno/Waves radio observations on the 2017/03/29.

Latitude and frequency distributions

- Latitude and frequency distributions between 2016 and 2019 (Louis et al., JGR, 2021):
  - nKOM and nLF distributions: **similar and complementary statistical structures**
  - **Minima of occurrence** of the nLF in the **low latitudes** explain its difficulty in being observed by missions prior to Juno.

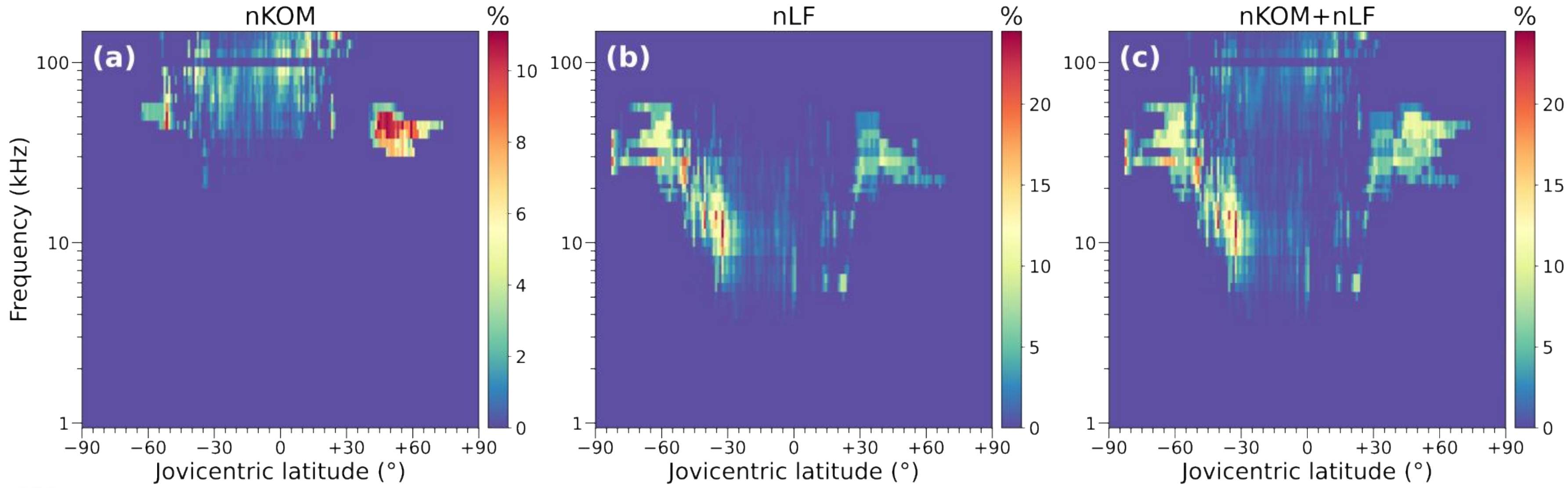

Latitude distributions and frequency of probability of occurrence of Juno-Wave observations of (a) nKOM, (b) nLF and (c) nKOM+nLF.

ÚSTAV FYZIKY ATMOSFÉRY AV ČR, v. v. i. LIRA Observatoire de Paris | PSL

Propagation of electromagnetic waves in plasmas

- Calculation of the refractive index of waves in plasma

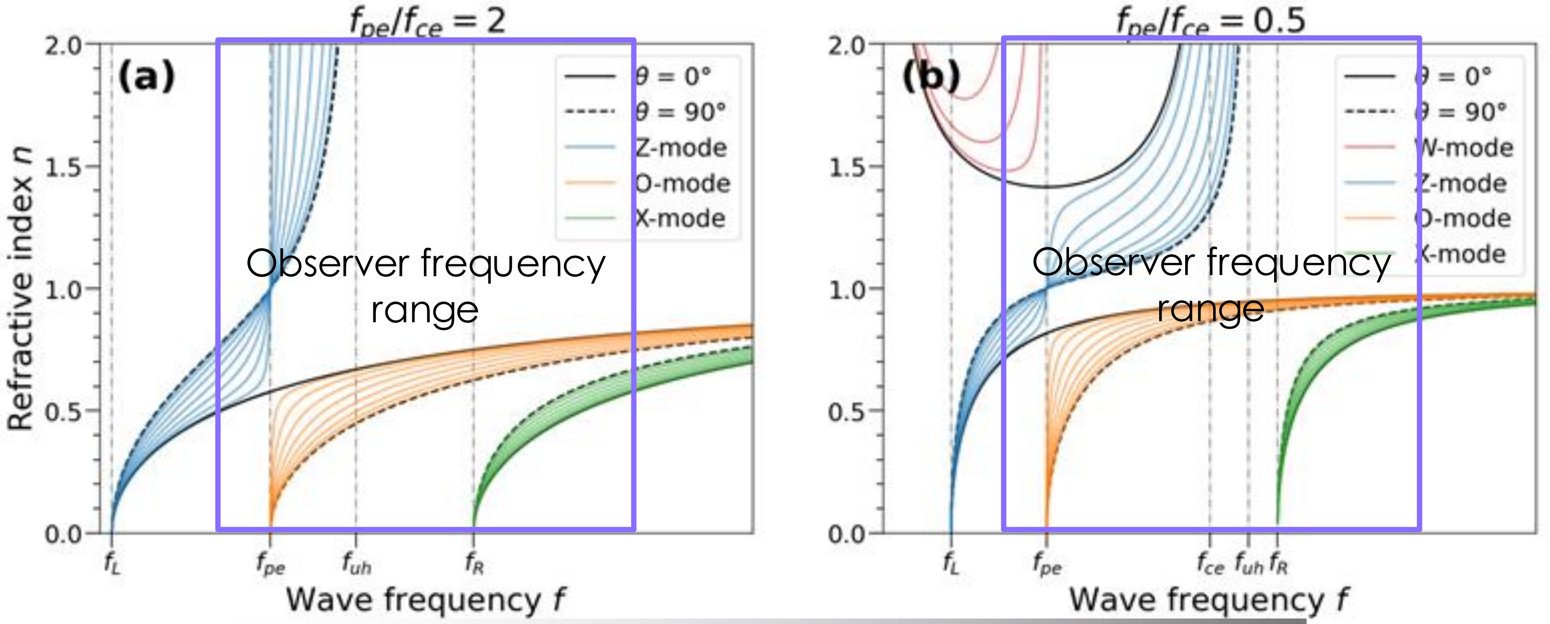

« **Trapped** » electromagnetic modes :
- Left-handed Extraordinary (Z-mode)
- *Whistler* (W-mode)

« **Free** » electromagnetic modes:
- Left-handed Ordinary (O-mode)
- Right-handed Extraordinary (X-mode)

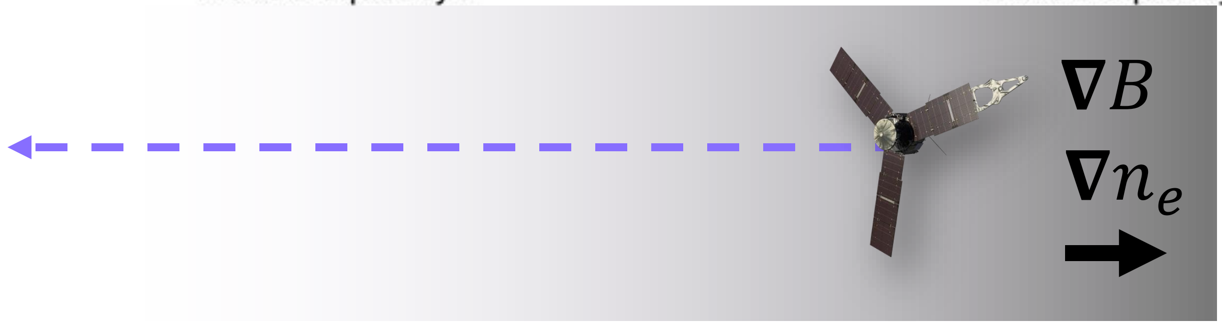

Mode Separation: Local Plasma Measurements with JADE and MAG

- Waves: no polarization measurements.

- Juno crossing of the plasma disk:
  - **JADE** : n_e measurements
  - **MAG** : $\mathbf{B}$ measurements
  - Calculation of $\boldsymbol{\omega_{pe}(n_e)}$ **et** $\boldsymbol{\omega_{ce}(B)}$: it is possible to constrain the **propagation mode according to 3 groups**:
    - **Trapped modes: ZW** (i.e., Z-mode or W-mode) : $\omega < \omega_{pe}$
    - **Free modes: XO** (i.e., X-mode or O-mode) : $\omega_{uh} < \omega$
    - **Undetermined mode: ZO** (i.e., Z-mode or O-mode) : $\omega_{pe} < \omega < \omega_{uh}$

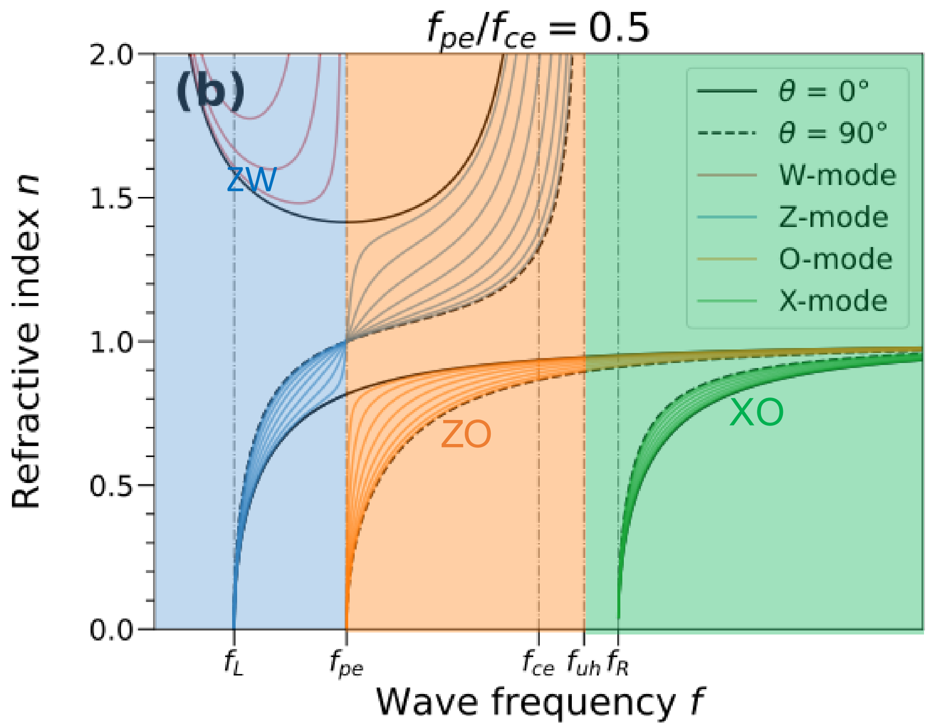

Mode separation: latitude and frequency distributions

- Exclusion of trapped observations (i.e., ZW)
- nKOM and nLF distributions of the propagation mode:
  - ZO-mode: nKOM and nLF are connected.
  - XO-mode: nKOM and nLF are disconnected.

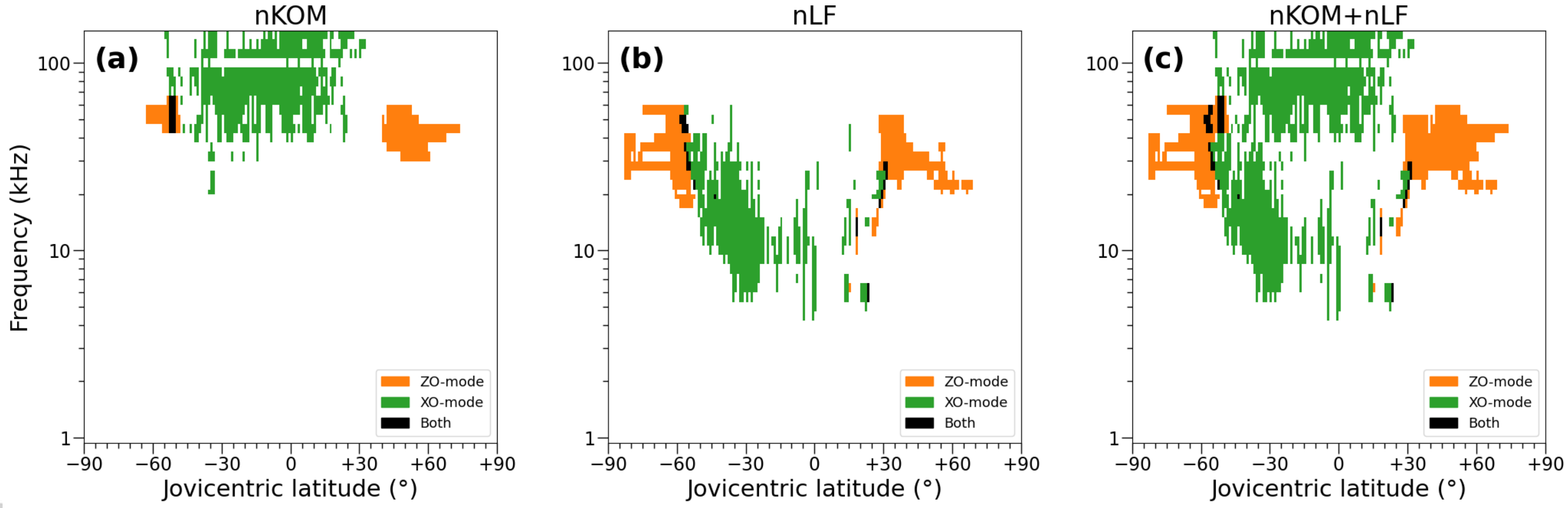

Latitude and frequency distributions of Juno-Wave observations of (a) nKOM, (b) nLF and (c) nKOM+nLF in XO (green) and ZO (orange).

ÚSTAV FYZIKY ATMOSFÉRY AV ČR, v. v. i. LIRA Observatoire de Paris | PSL

LsPRESSO : Large-scale Plasma Radio Emissions Simulation of Spacecraft Observations

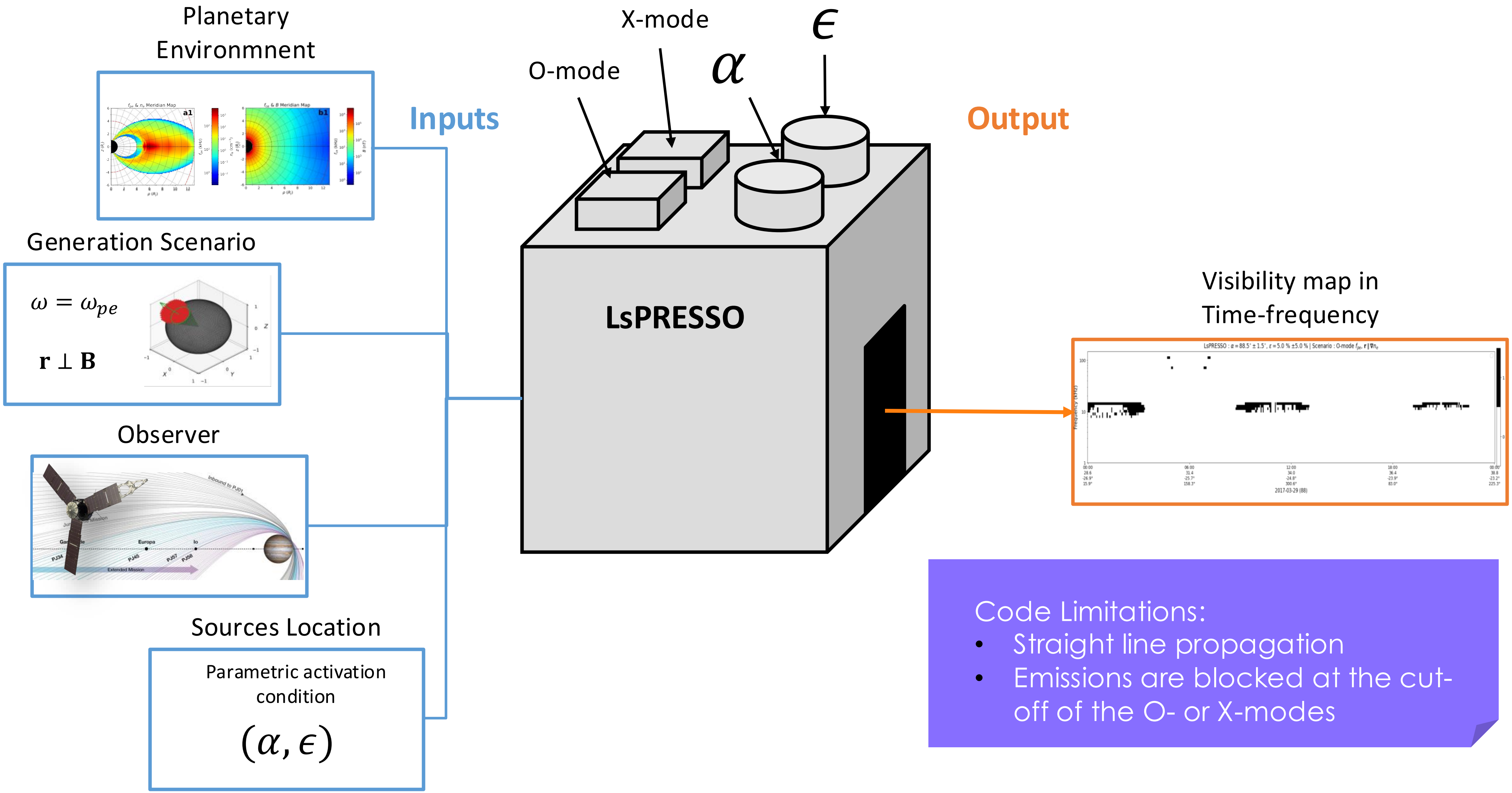

Code Limitations:
- Straight line propagation
- Emissions are blocked at the cut-off of the O- or X-modes

Initialization : Simulation of the Juno observations

- Sources location:
  - We choose to constraint them with 2 parameters :
    - $\alpha = \angle(\boldsymbol{\nabla} n_e, \mathbf{B})$, with $\alpha \in [0°, 90°]$ by 3° steps
    - $\epsilon = \text{centile}(||\boldsymbol{\nabla} n_e||)$, with $\epsilon \in [0\%, 100\%]$ by 10% steps
  - Since there is no reliable model on intermittency, **active sources are assumed to be permanent**.

- Generation scenarios:

Scenario #1 :
Jones (1980)

Frequency:

$$\omega = \omega_{pe}$$

Directivity:

$$\angle(\mathbf{r}_{\pm}, \mathbf{B}) = \frac{\pi}{2} \mp \left(\frac{\pi}{2} - \beta\right)$$

Scenario #2 :
Fung & Papadopoulos (1987)

Frequency:

$$\omega = 2\omega_{uh}$$

Directivity:

$$\mathbf{r} \perp \mathbf{B}$$

Scenario #3 :
Aligned with -$\boldsymbol{\nabla} n_e$ at ω_{pe}

Frequency:

$$\omega = \omega_{pe}$$

Directivity:

$$\mathbf{r} \parallel -\boldsymbol{\nabla} n_e$$

Scenario #4 :
Aligned with -$\boldsymbol{\nabla} n_e$ at $2\omega_{pe}$

Frequency:

$$\omega = 2\omega_{pe}$$

Directivity:

$$\mathbf{r} \parallel -\boldsymbol{\nabla} n_e$$

$$\beta = \arctan\left(\sqrt{\frac{\omega_{pe}}{\omega_{ce}}}\right)$$

ÚSTAV FYZIKY ATMOSFÉRY
AV ČR, v. v. i.
LIRA Observatoire de Paris | PSL

Initialization : Simulation of the Juno observations

- Sources location:
  - We choose to constraint them with 2 parameters :
    - $\alpha = \angle(\nabla n_e, \mathbf{B})$, with $\alpha \in [0°, 90°]$ by 3° steps
    - $\epsilon = \text{centile}(||\nabla n_e||)$, with $\epsilon \in [0\%, 100\%]$ by 10% steps
  - Since there is no reliable model on intermittency, **active sources are assumed to be permanent**.

- Generation scenarios:

Scenario #1 : Jones (1980)	Scenario #2 : Fung & Papadopoulos (1987)	Scenario #3 : Aligned with -∇n_e at ω_{pe}	Scenario #4 : Aligned with -∇n_e at $2\omega_{pe}$
Frequency: $\omega = \omega_{pe}$	Frequency: $\omega = 2\omega_{uh}$	Frequency: $\omega = \omega_{pe}$	Frequency: $\omega = 2\omega_{pe}$
Directivity: $\angle(\mathbf{r}_\pm, \mathbf{B}) = \frac{\pi}{2} \mp \left(\frac{\pi}{2} - \beta\right)$	Directivity: $\mathbf{r} \perp \mathbf{B}$	Directivity: $\mathbf{r} \parallel -\nabla n_e$	Directivity: $\mathbf{r} \parallel -\nabla n_e$
Incompatible with the nKOM and nLF observations	Only compatible with the nKOM observation in XO	Compatible with the nKOM and nLF observations	Compatible with the nKOM and nLF observations

Results : Generation scenarios compatible with the nKOM

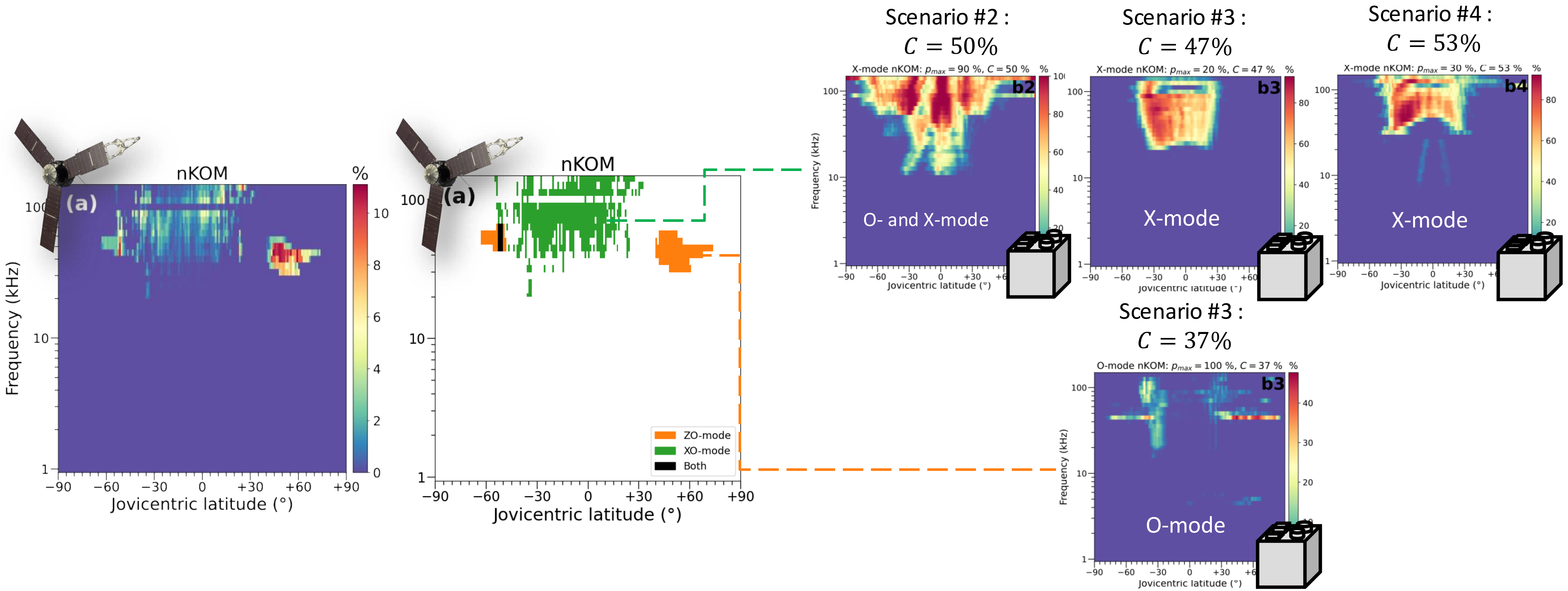

Results : Predicted sources distribution for the nKOM

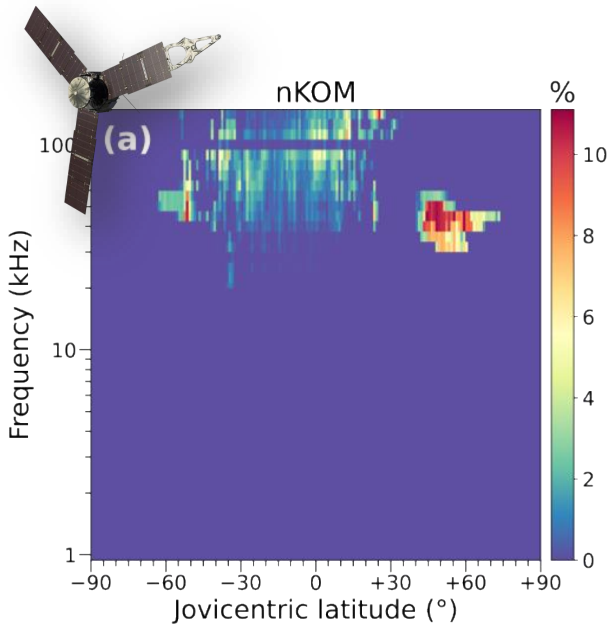

Scenario #2 : Scenario #3 : Scenario #4 :

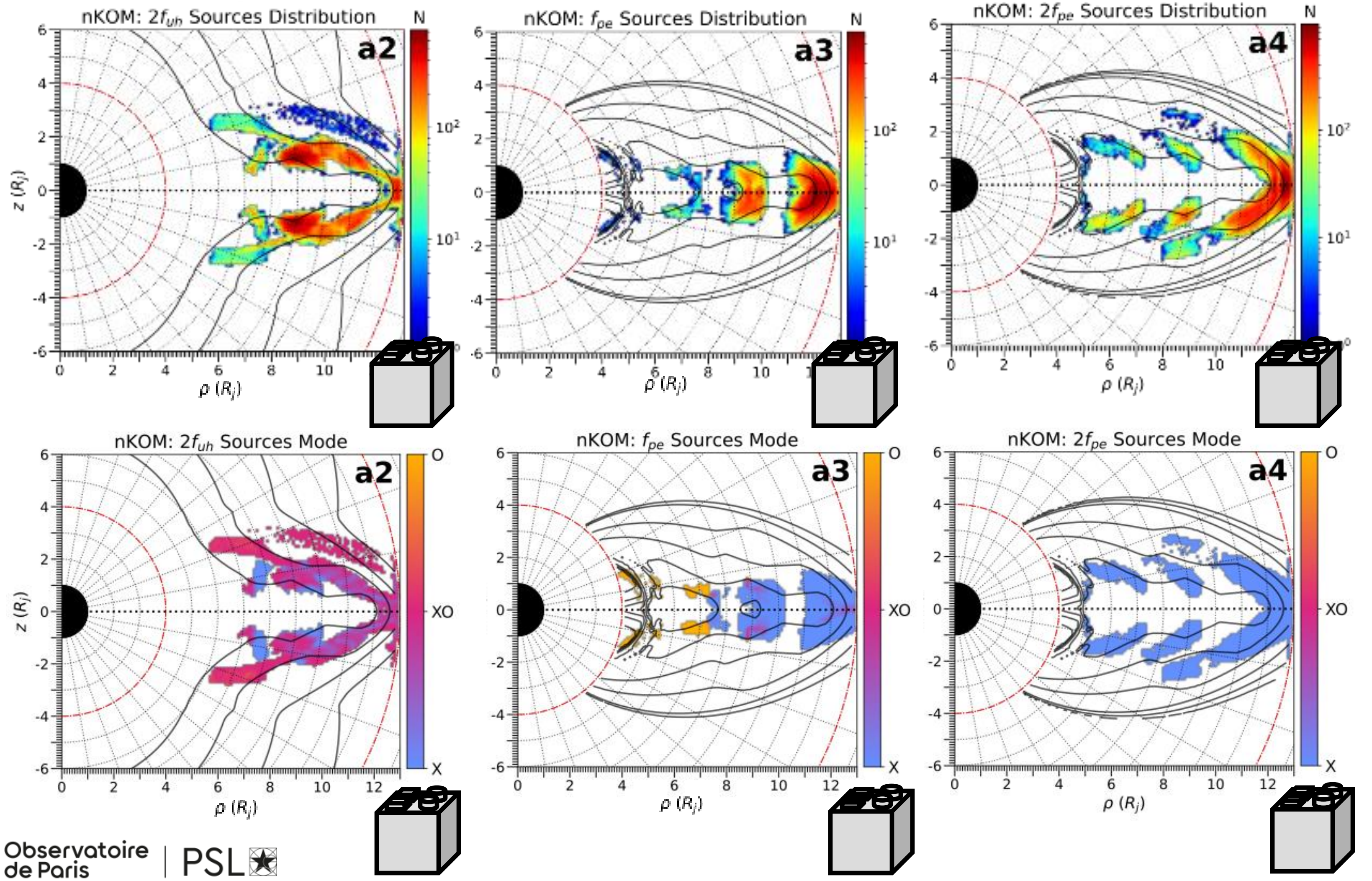

Results : Generation scenarios compatible with the nLF

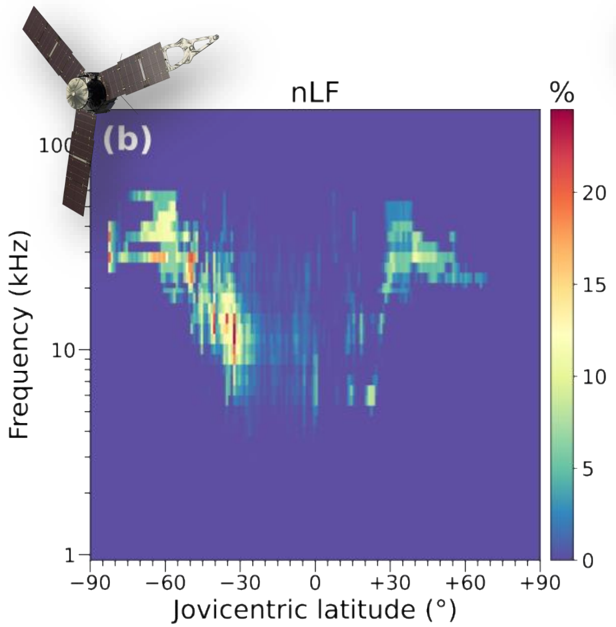

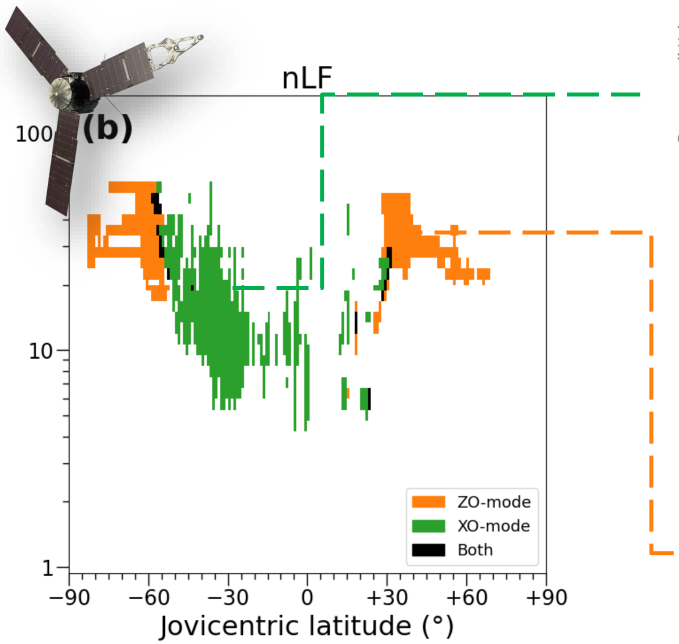

Scenario #3 :
$C = 48\%$

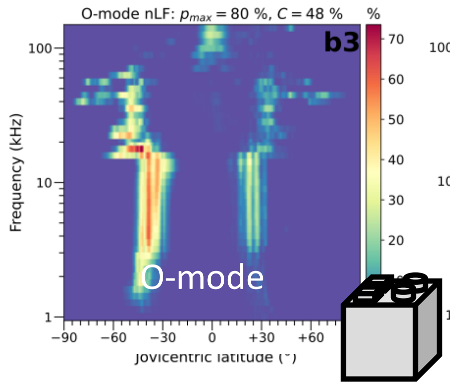

Scenario #4 :
$C = 45\%$

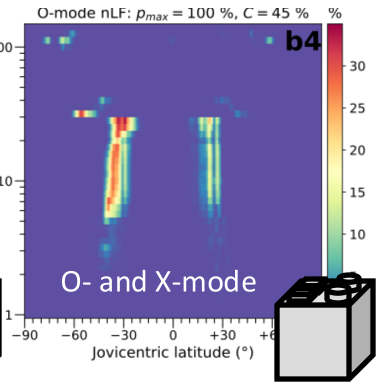

Scenario #4 :
$C = 55\%$

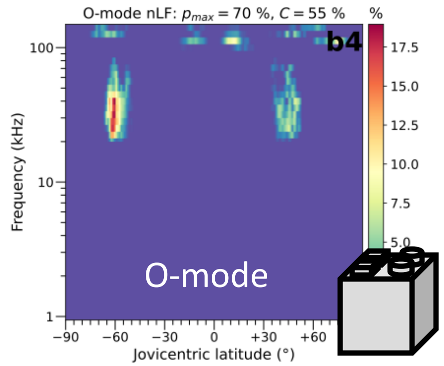

Results : Predicted sources distribution for the nLF

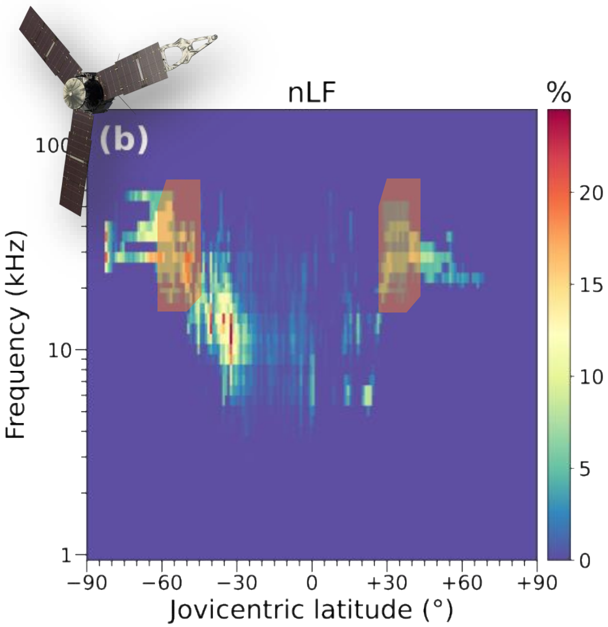

Scenario #3 :

Scenario #4 :

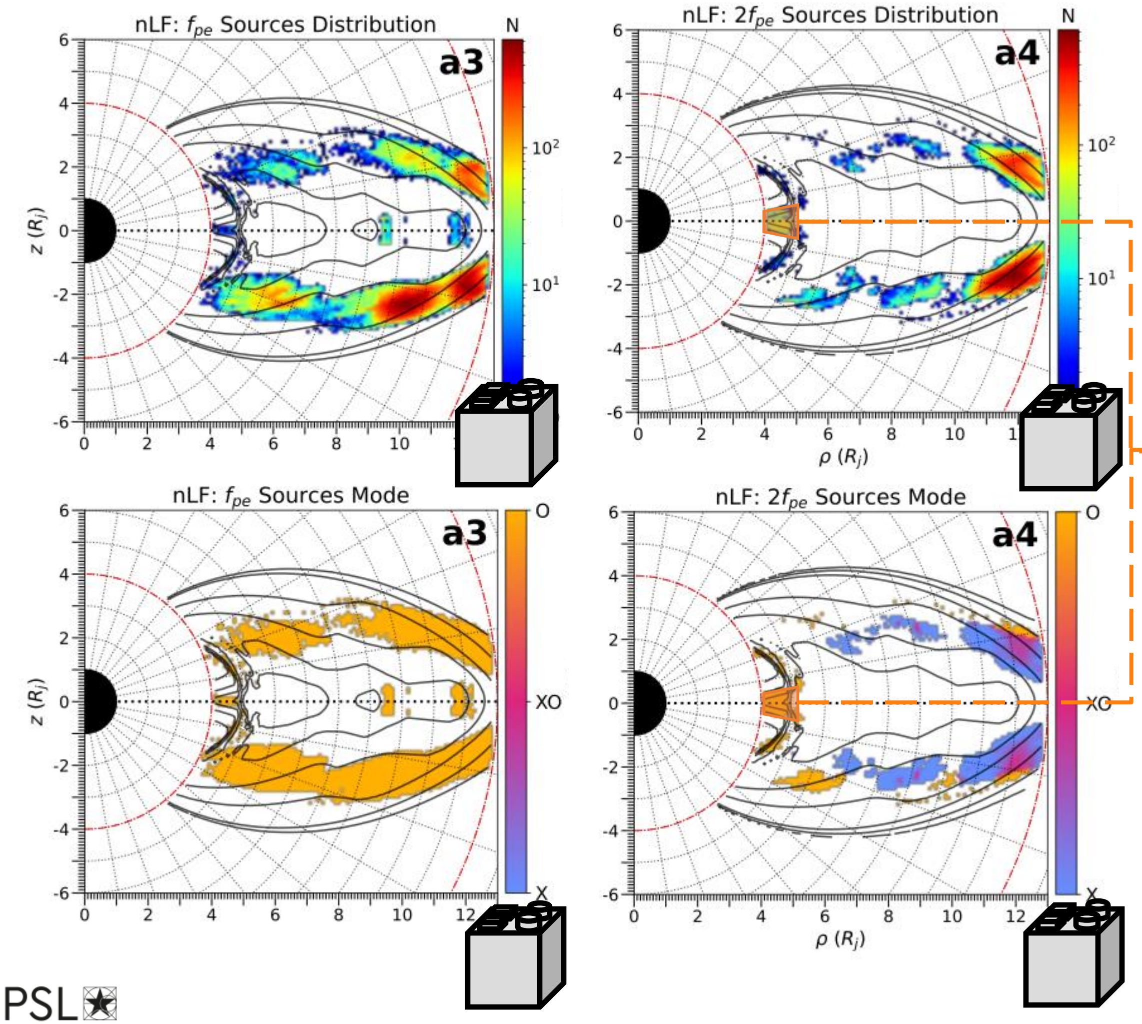

Scenario #4 :

$C = 55\%$

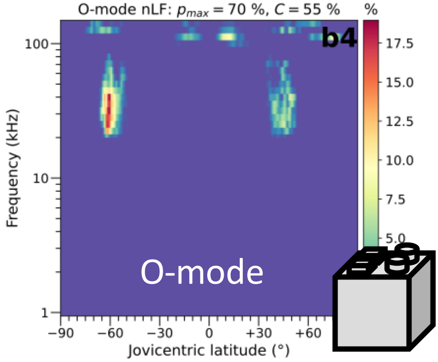

Summary : generation and location of the jovian plasma emissions

- nKOM :
  - **XO** : It is difficult to constrain the characteristics of the emissions, but simulations suggest its cut-off in **X-mode.**
  - **ZO** : Compatible with a generation at ω_{pe} **for the** $\alpha \sim 55.5^\circ \pm 1.5^\circ$.
- nLF :
  - **XO** : Compatible with a generation at ω_{pe} **and** $2\omega_{pe}$ **in the regions where** $\alpha > 75^\circ$ **(i.e.,** $\nabla n_e \perp \mathbf{B}$**)**
  - **ZO** :
    - Partly compatible with a generation at ω_{pe} **in the regions where** $\alpha > 75^\circ$ **(i.e.,** $\nabla n_e \perp \mathbf{B}$**)**
    - Partly compatible with a generation at $2\omega_{pe}$ **in the regions where** $\alpha < 15^\circ$ **(i.e,** $\nabla n_e \parallel \mathbf{B}$**).**

$\alpha = \angle(\nabla n_e, \mathbf{B})$
$\epsilon = \text{centile}(||\nabla n_e||)$

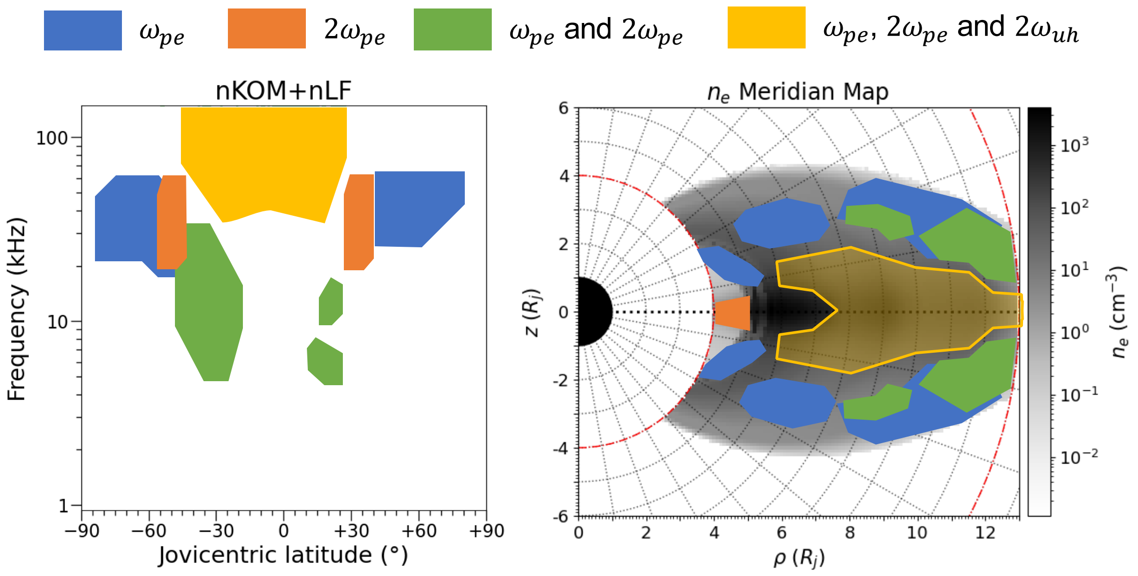

LsPRESSO : Comparison with the nLF observations of the PJ01

- Imai et al. (2017) : nKOM and nLF sources locations for the Juno-Waves observations near the flyby of the PJ01.

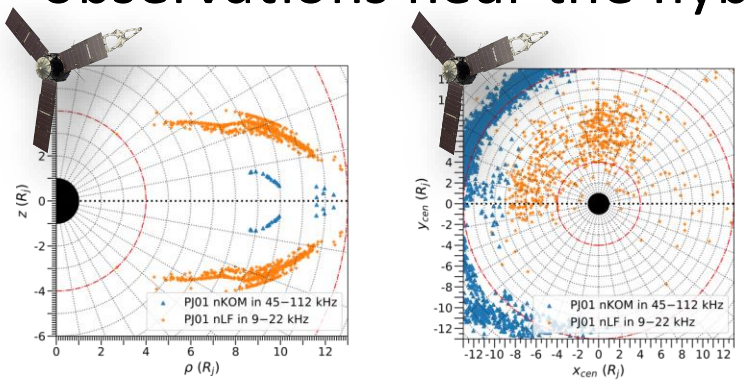

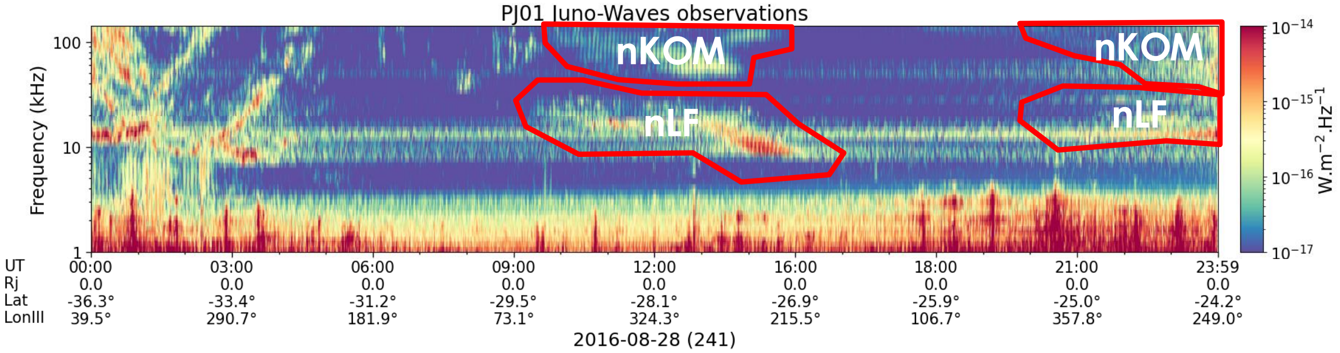

ÚSTAV FYZIKY ATMOSFÉRY AV ČR, v. v. i. | LIRA | Observatoire de Paris | PSL

LsPRESSO : Comparison with the nLF observations of the PJ01

- Imai et al. (2017) : nKOM and nLF sources locations for the Juno-Waves observations near the flyby of the PJ01.

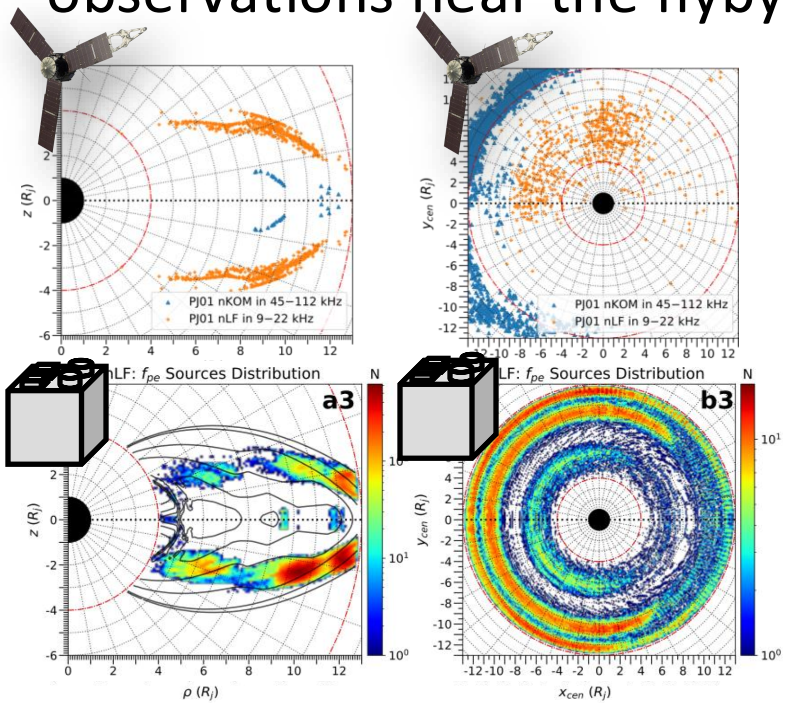

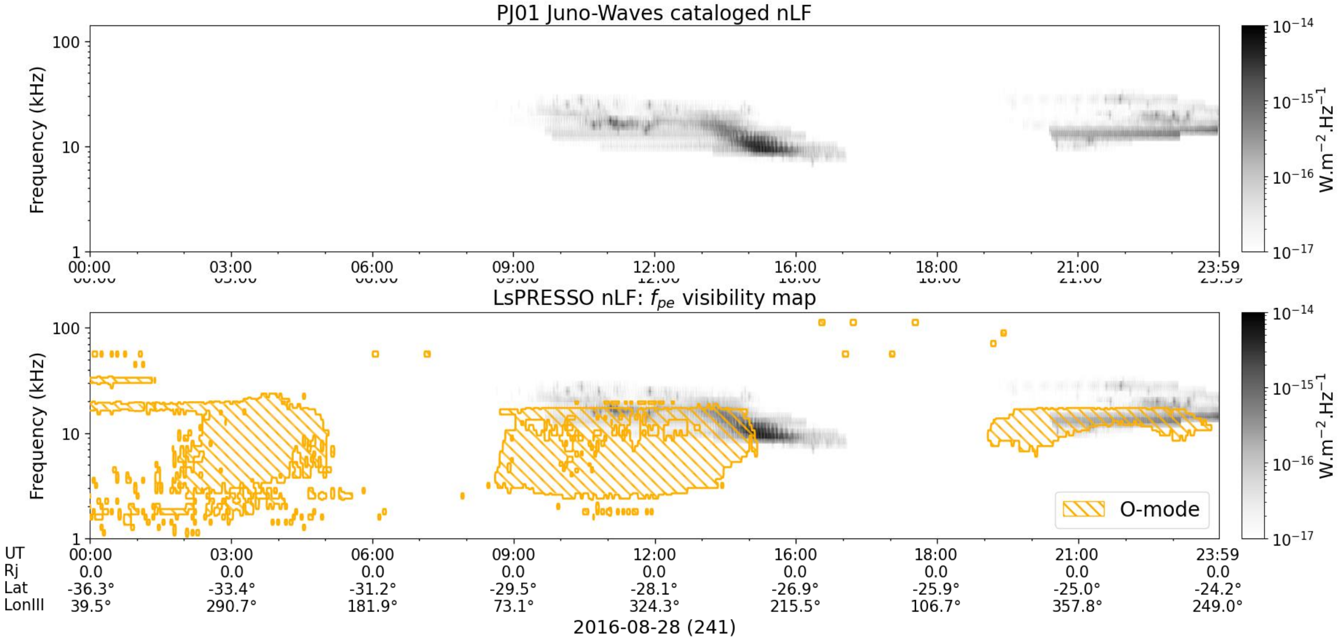

ÚSTAV FYZIKY ATMOSFÉRY AV ČR, v. v. i.
LIRA
Observatoire de Paris | PSL

LsPRESSO : Comparison with the nLF observations of the PJ01

- Imai et al. (2017) : nKOM and nLF sources locations for the Juno-Waves observations near the flyby of the PJ01.

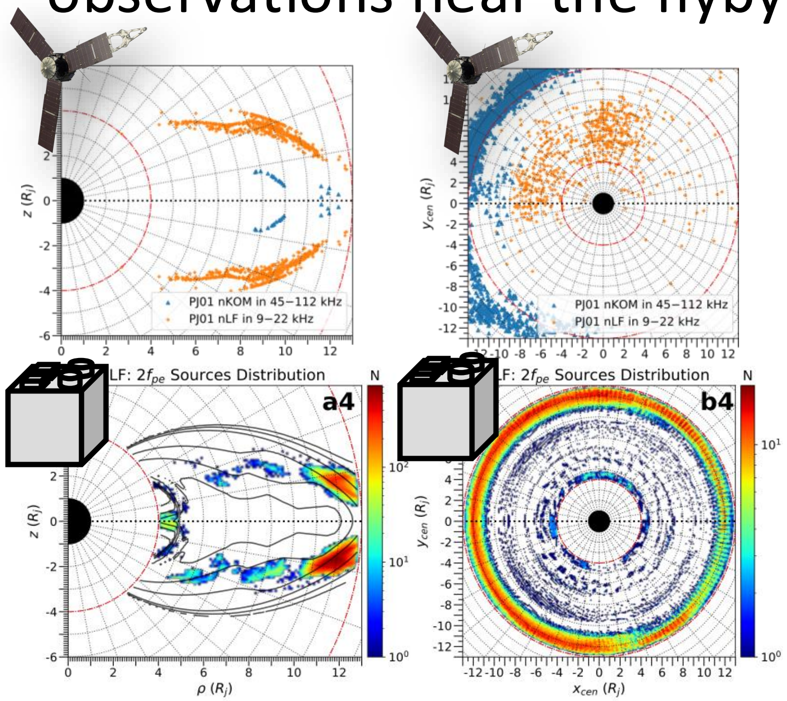

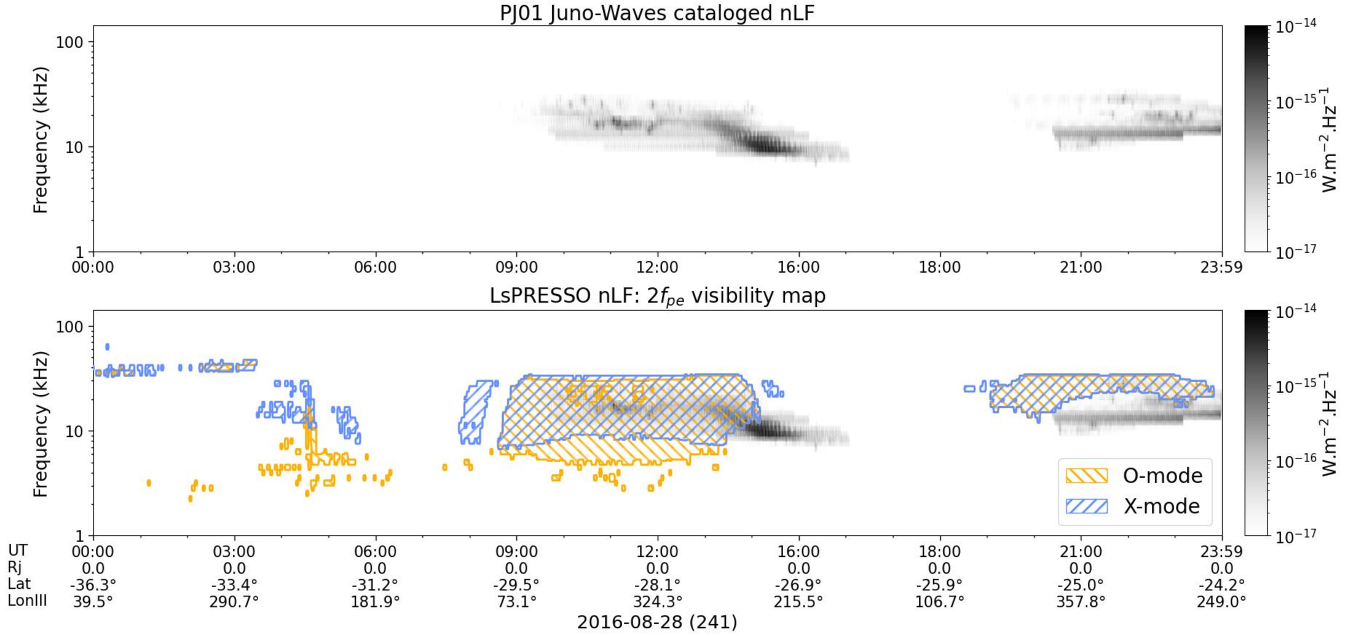

Thank you for your attention !

Conclusion

- It is possible to constraint planetary plasma emissions using the geometrical statistics of spacecraft observations.
- Simulation of spacecraft observation with LsPRESSO :
  - **Allow to deduce constrain the generation and the location of the radio sources**.
  - **Capable to reproduce** the visibility of the emissions in the time-frequency plane
- New constraints on the nKOM and the nLF.
- Articles :
  - Study on the nKOM : published [Boudouma et al., JGR, 2024]
  - Study on the nKOM & the nLF + propagation modes : about to be submitted [Boudouma et al., JGR, 2025]

ÚSTAV FYZIKY ATMOSFÉRY AV ČR, v. v. i. LIRA Observatoire de Paris | PSL

LsPRESSO: generation and location of the saturnian plasma emissions

- Application of the method for the study of plasma emissions from Saturn:
    - *Cassini*-RPWS observations: **Similarities of Saturn's narrowband (NB) emissions to nKOM and nLF**
    - Application of the presented study to the Cassini-RPWS observations (flux and polarisation)

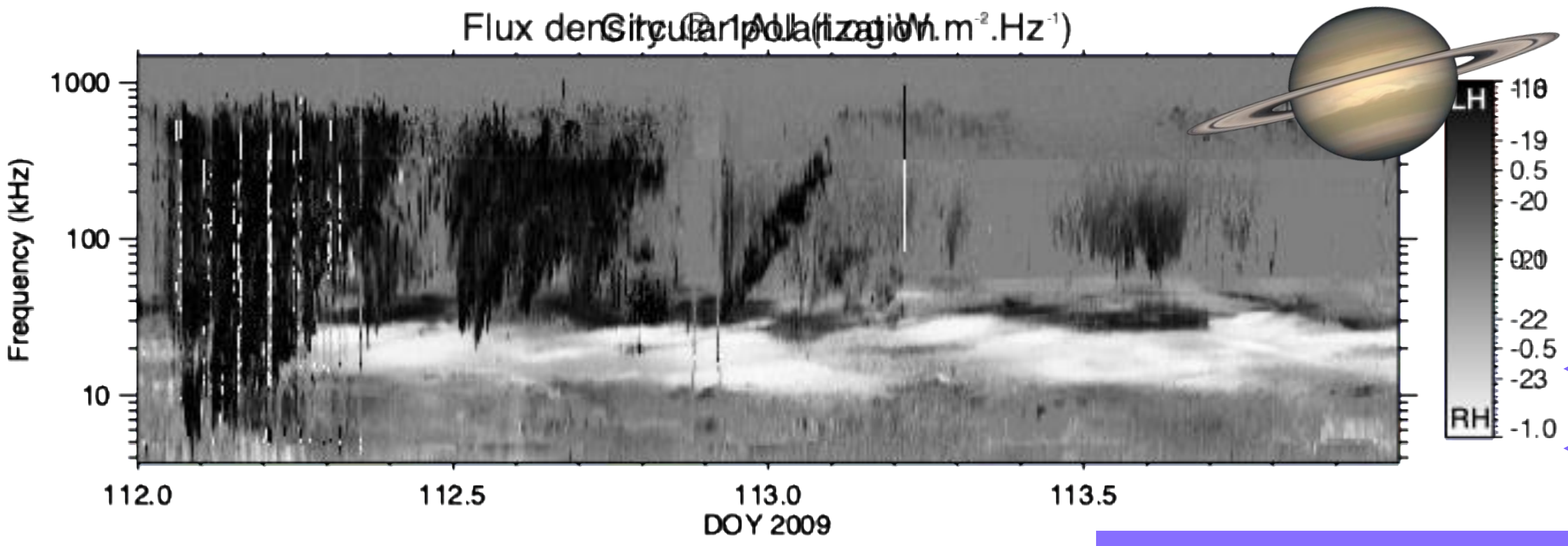

NB at 20 kHz

NB at 5 kHz

Dynamic spectrum of 48 hours of radio observations in Saturn's magnetosphere with Cassini-RPWS

nKOM and nLF observations history

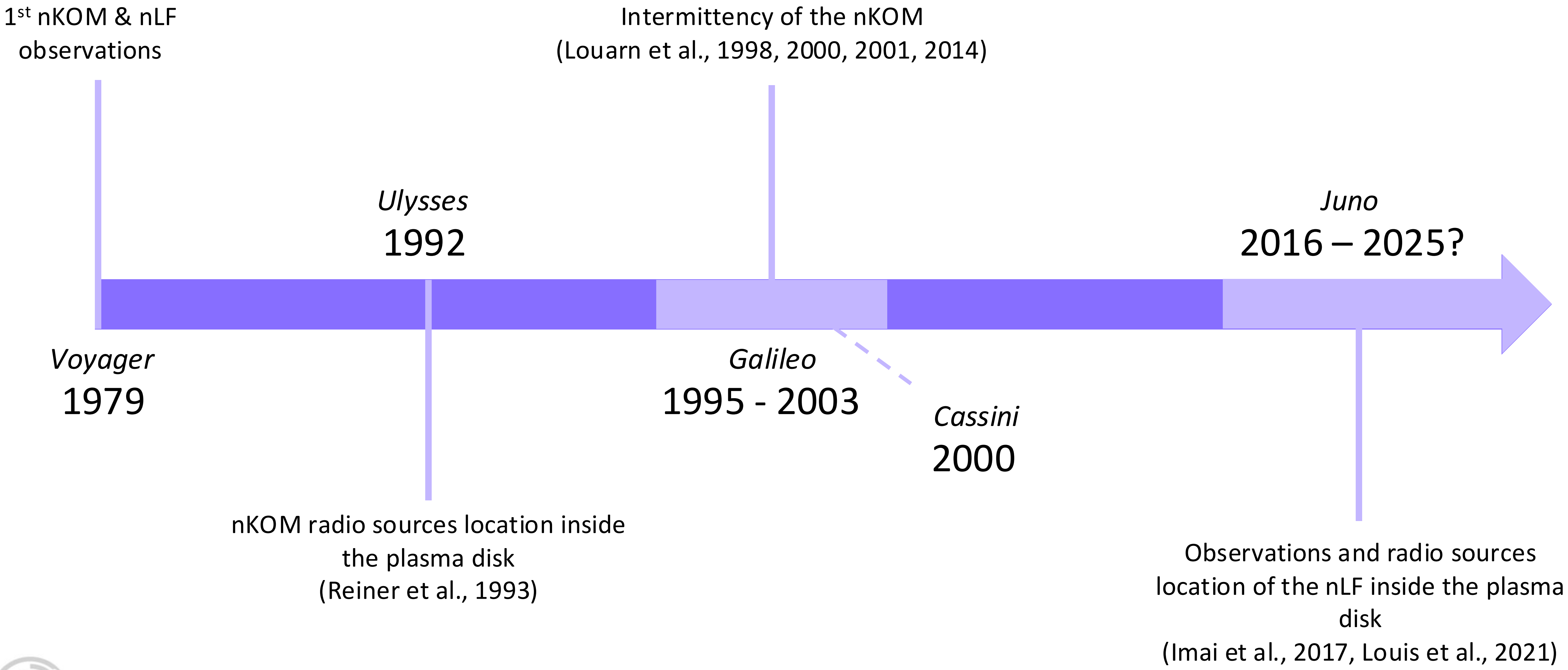

ÚSTAV FYZIKY ATMOSFÉRY AV ČR, v. v. i. LIRA Observatoire de Paris | PSL

Radio observations with the Waves instrument

- Constitution of the Juno-Waves radio observations database:
  - **Calibration** of the radio signal measured by the **Waves instrument**(Louis et al., JGR, 2021)
  - **Participation in the development of the SPACE cataloguing tool** (Louis et al., 2022)
  - **Extension of the Jovian radio component catalog (formerly covering 2016-2019)** until the beginning of **2023** (Boudouma et al., 2024).

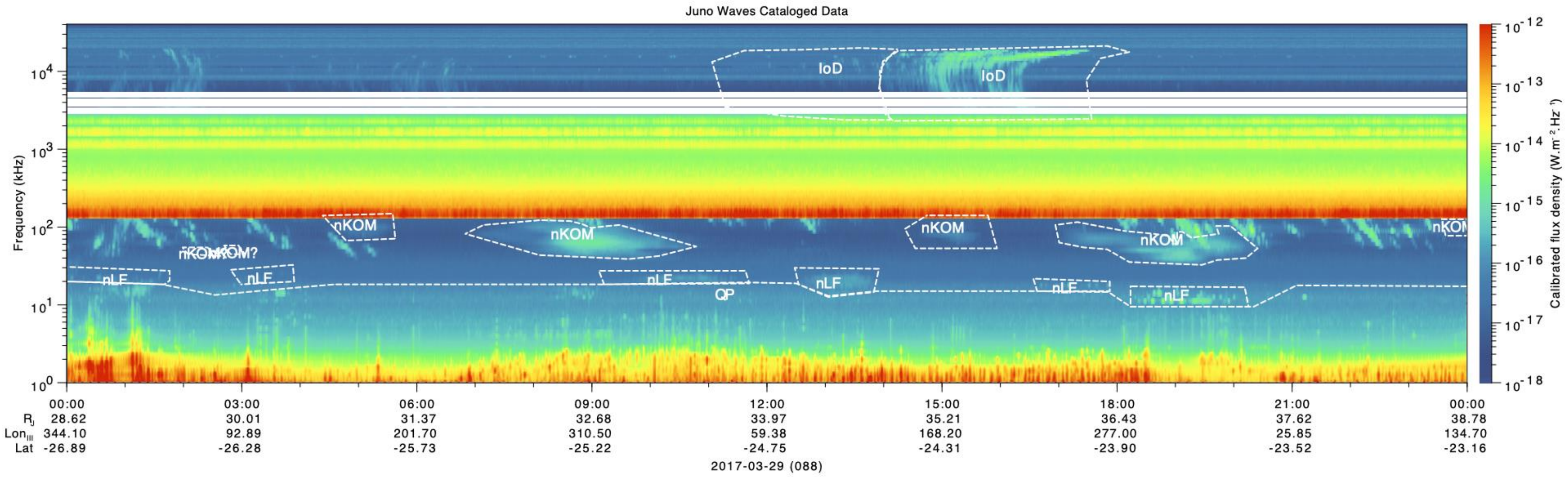

ÚSTAV FYZIKY ATMOSFÉRY AV ČR, v. v. i. LIRA SORBONNE UNIVERSITÉ Observatoire de Paris | PSL

Characteristic frequencies of electrostatic waves

- In plasmas, the dynamics of charged particles are coupled with the electric fields **E** and magnetic fields **B**:
  - **Collective motions of particles** in the form of waves of matter, called **electrostatic waves**
  - **In magnetized plasmas**, these electrostatic waves are described according to **2 characteristic frequencies**:

Electric Force:
The "plasma" oscillation

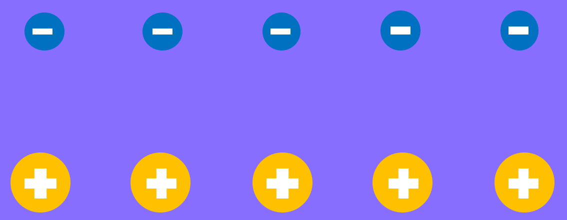

$$\omega_p = \sqrt{\frac{ne^2}{m\varepsilon_0}}$$

Magnetic Force:
cyclotron gyration

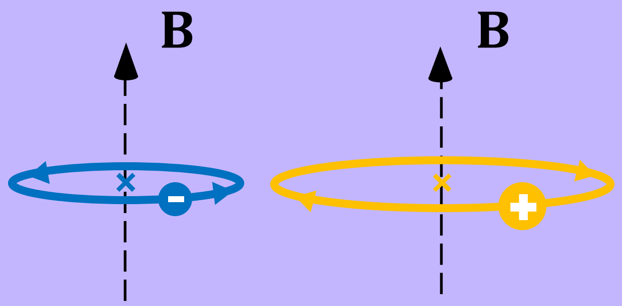

$$\omega_c = \frac{eB}{m}$$

Linear Mode Conversion Mechanisms

- Inhomogeneous plasma:
  - Energy transfer from **trapped modes (W or Z) to free modes (O or X)** at $\boldsymbol{\omega \sim \omega_{pe}}$

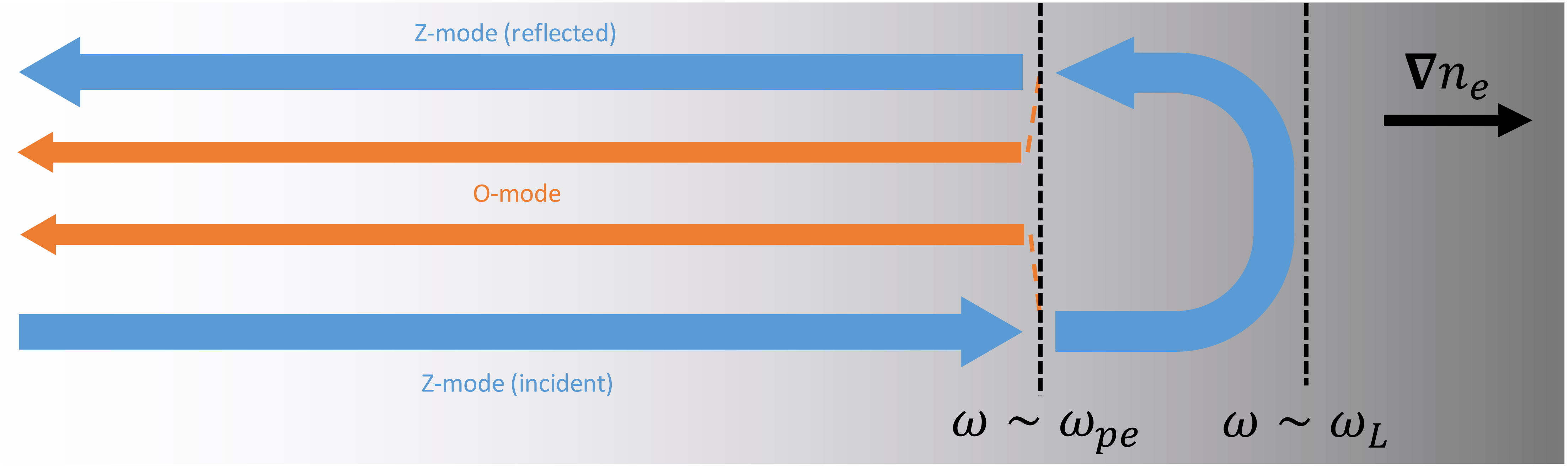

Example of linear conversion of a wave in Z-mode to O-mode.

Nonlinear mode conversion mechanisms: three-wave coupling

- Homogeneous or inhomogeneous plasma:
  - **In space plasmas,** electrostatic waves, **called Langmuir waves, can convert to electromagnetic waves in O- and X-mode at $\omega \sim \omega_{pe}$ and $\omega \sim 2\omega_{pe}$** through the **3-wave coupling process.**

Step 1 : Langmuir wave decay

$$\underset{\omega \sim \omega_{pe}}{L} \longrightarrow \underset{\omega \sim \omega_{pe}}{L'} + \underset{\omega \ll \omega_{pe}}{S}$$

Step 2 : Langmuir wave coalescence

$$\underset{\omega \sim \omega_{pe}}{L} + \underset{\omega \ll \omega_{pe}}{S} \longrightarrow \underset{\omega \sim \omega_{pe}}{T_{\omega_{pe}}}$$

$$\underset{\omega \sim \omega_{pe}}{L} + \underset{\omega \sim \omega_{pe}}{L'} \longrightarrow \underset{\omega \sim 2\omega_{pe}}{T_{2\omega_{pe}}}$$

Génération des ondes électrostatiques dans les plasmas spatiaux

- Les ondes électrostatiques émergent des instabilités du plasma :
  - Les oscillations « plasma », aussi appelées, **ondes de Langmuir**, sont générées suivant **l'instabilité faisceau-plasma** (ou « *bump-on-tail* »).

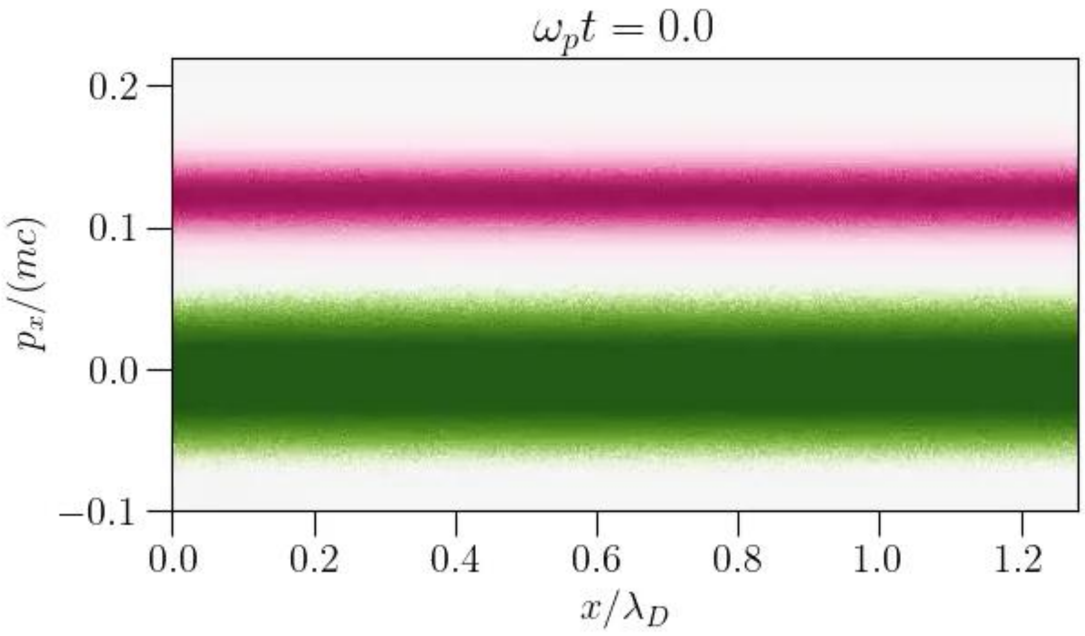

Simulation PIC 1D de l'instabilité faisceau plasma :
- En vert : la population d'électrons du plasma
- En rose : la population d'électrons du faisceau de densité plus faible et de vitesse positive relativement à celle du plasma

Source : Chaîne YouTube de la Fédération PLAS@PAR, « *Kinetic simulation of the bump-on-tail instability* »

ÚSTAV FYZIKY ATMOSFÉRY AV ČR, v. v. i. LIRA Observatoire de Paris | PSL

Propagation of electromagnetic waves in plasmas

- Calculation of the refractive index of waves in plasma

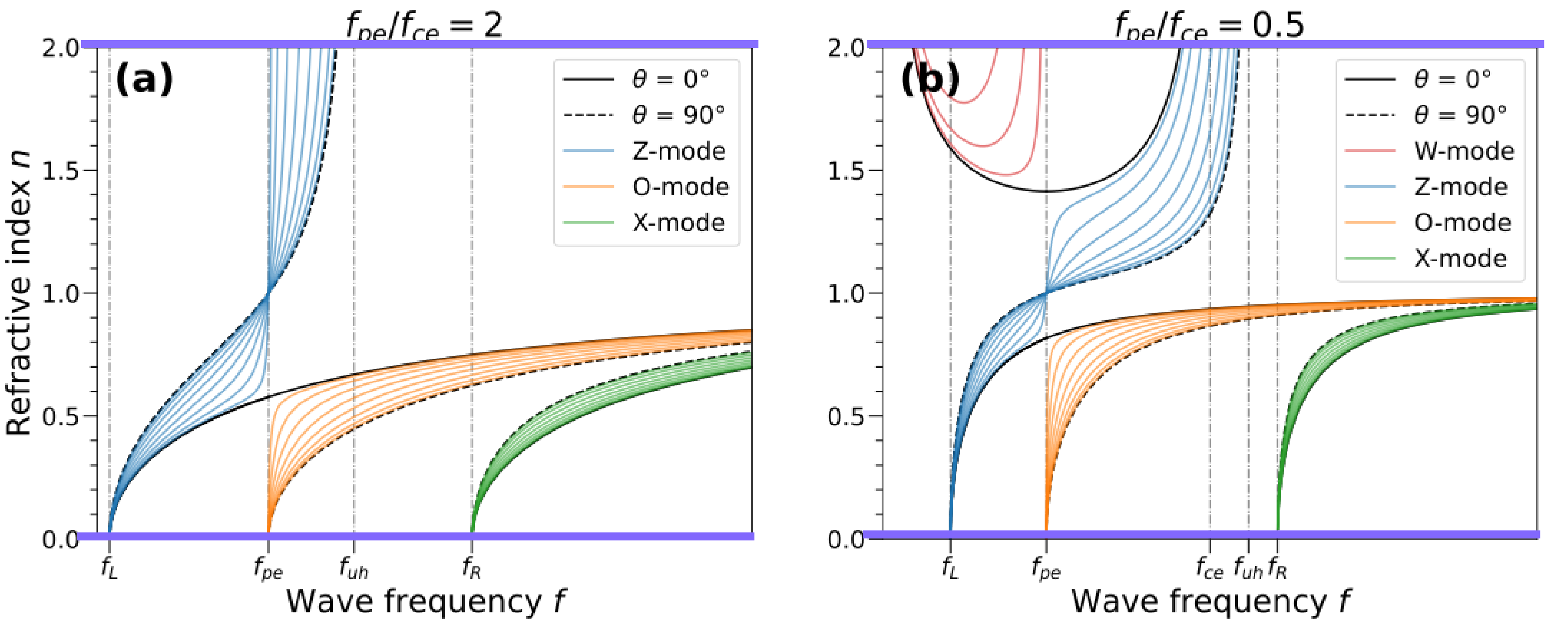

When N →∞:
- **Resonance frequency:** absorption by the plasma

When $N \rightarrow 0$:
- **Cut-off frequency** : reflexion by the plasma

$$\omega_{pe} = \sqrt{\frac{n_e e^2}{m_e \varepsilon_0}} \qquad \omega_{ce} = \frac{eB}{m_e} \qquad f = \frac{\omega}{2\pi}$$

Plasma emission generation: non-linear conversion of Langmuir waves

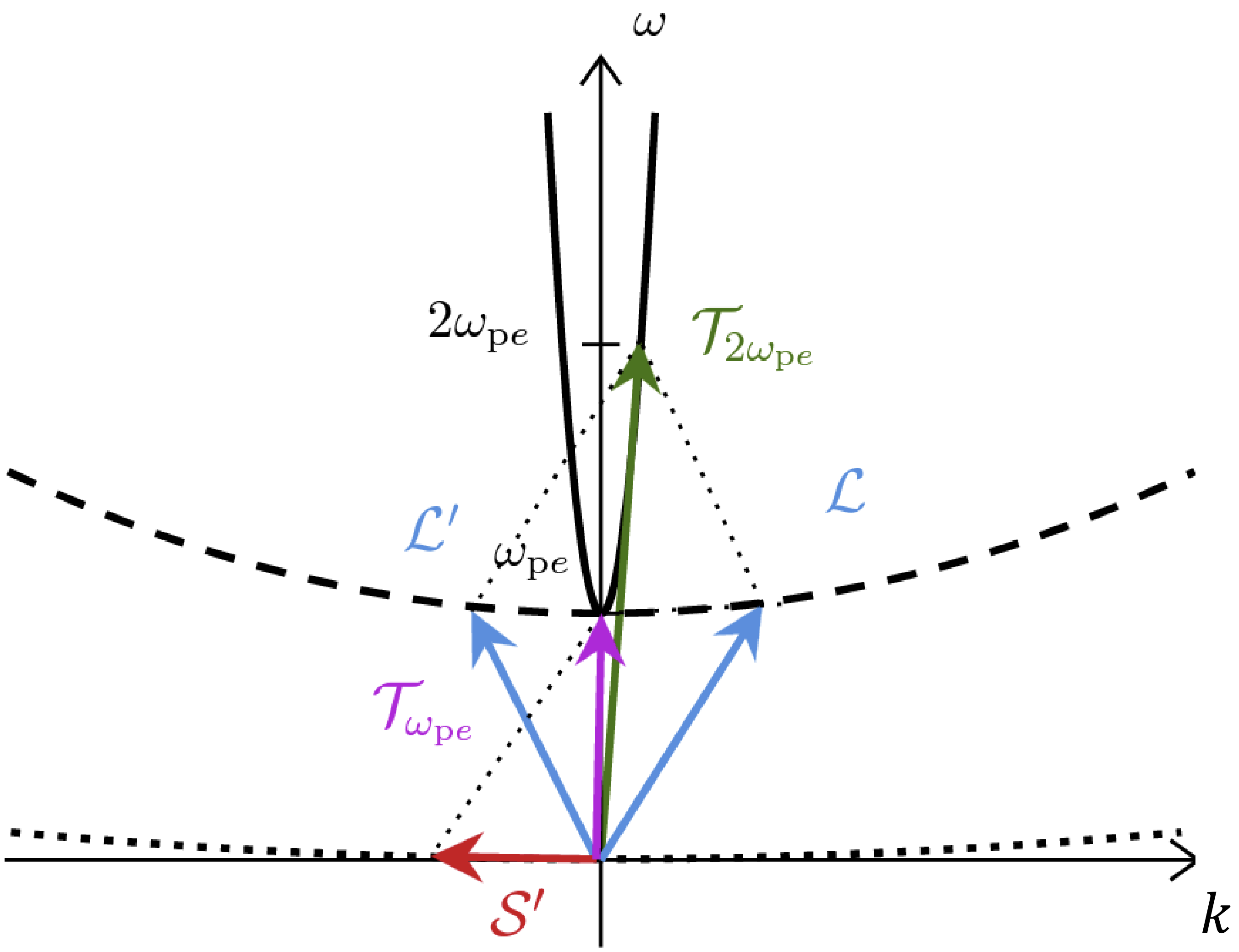

Schéma de conversion non-linéaire d'ondes de Langmuir en ondes électromagnétiques à ω_{pe} et $2\omega_{pe}$ (Gauthier, 2023)

Latitude and frequency distributions of the Jovian radio components (Louis et al. 2021)

Plasma Emissions

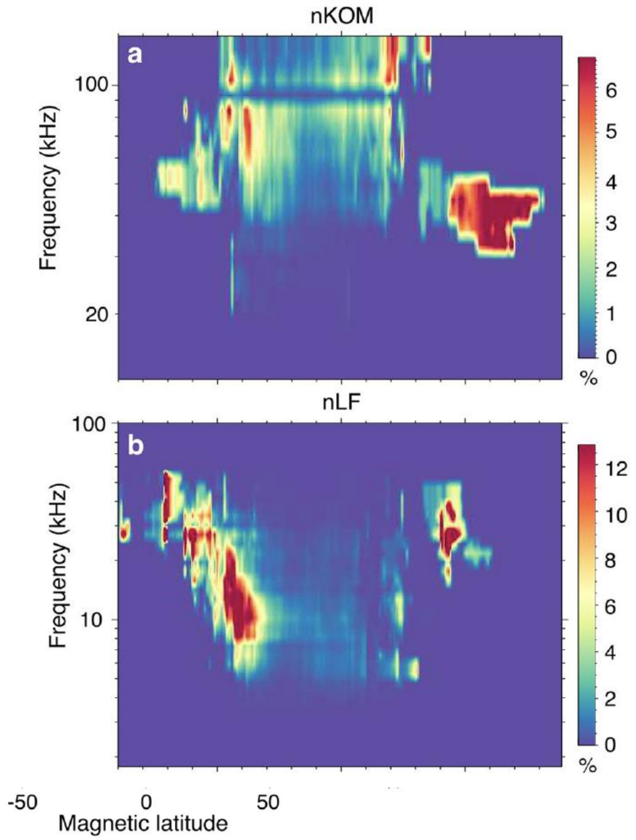

Maser-cyclotron Emissions

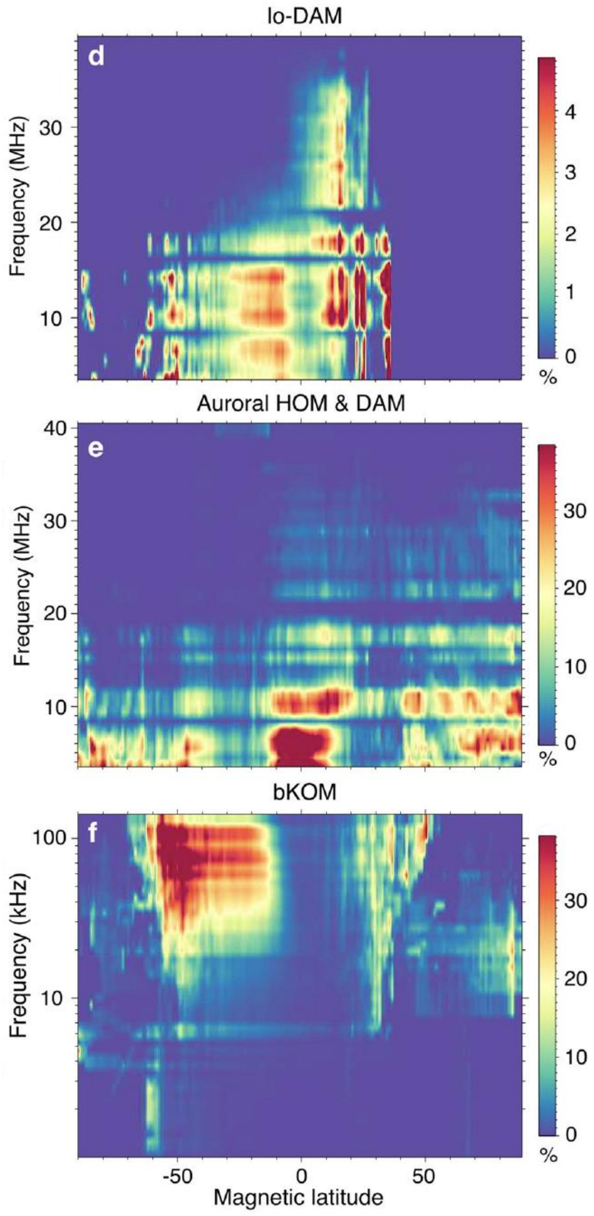

ÚSTAV FYZIKY ATMOSFÉRY
AV ČR, v. v. i.
LIRA Observatoire de Paris | PSL

Intermittency of the nKOM (Louarn et al., 1998, 2000, 2001, 2014)

nKOM sources activation

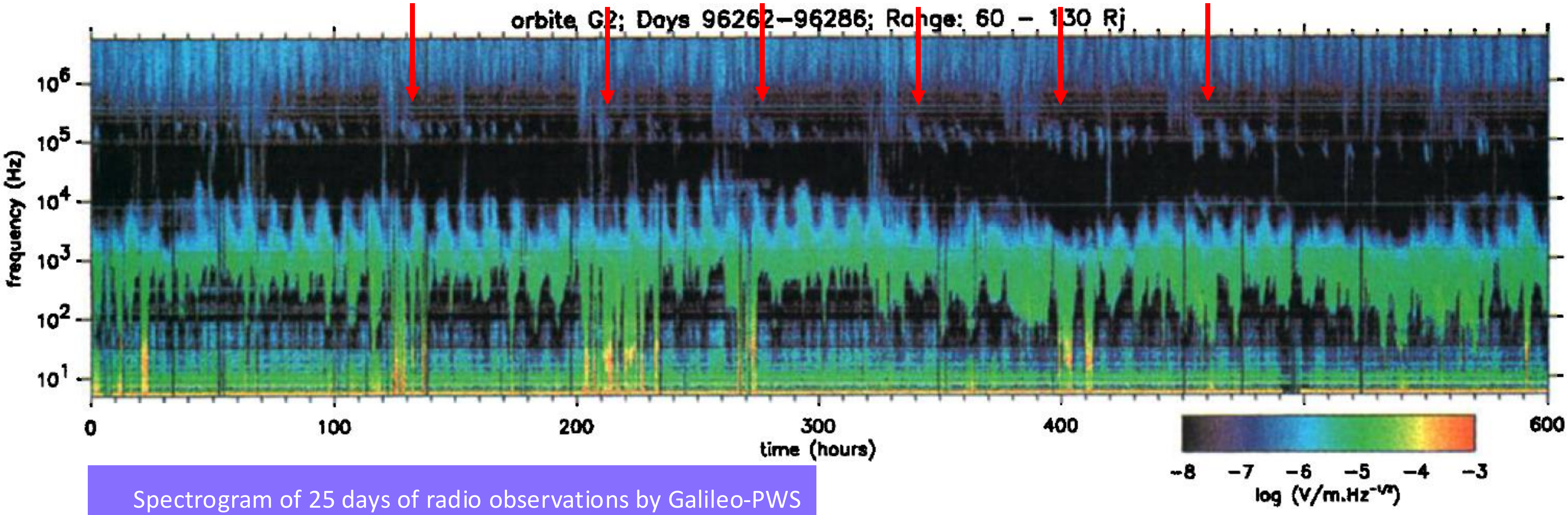

Spectrogram of 25 days of radio observations by Galileo-PWS between 18/09/1996 and 12/10/1996 (Louarn et al. 1998)

ÚSTAV FYZIKY ATMOSFÉRY AV ČR, v. v. i. LIRA Observatoire de Paris | PSL

Mode separation: latitude and frequency distributions

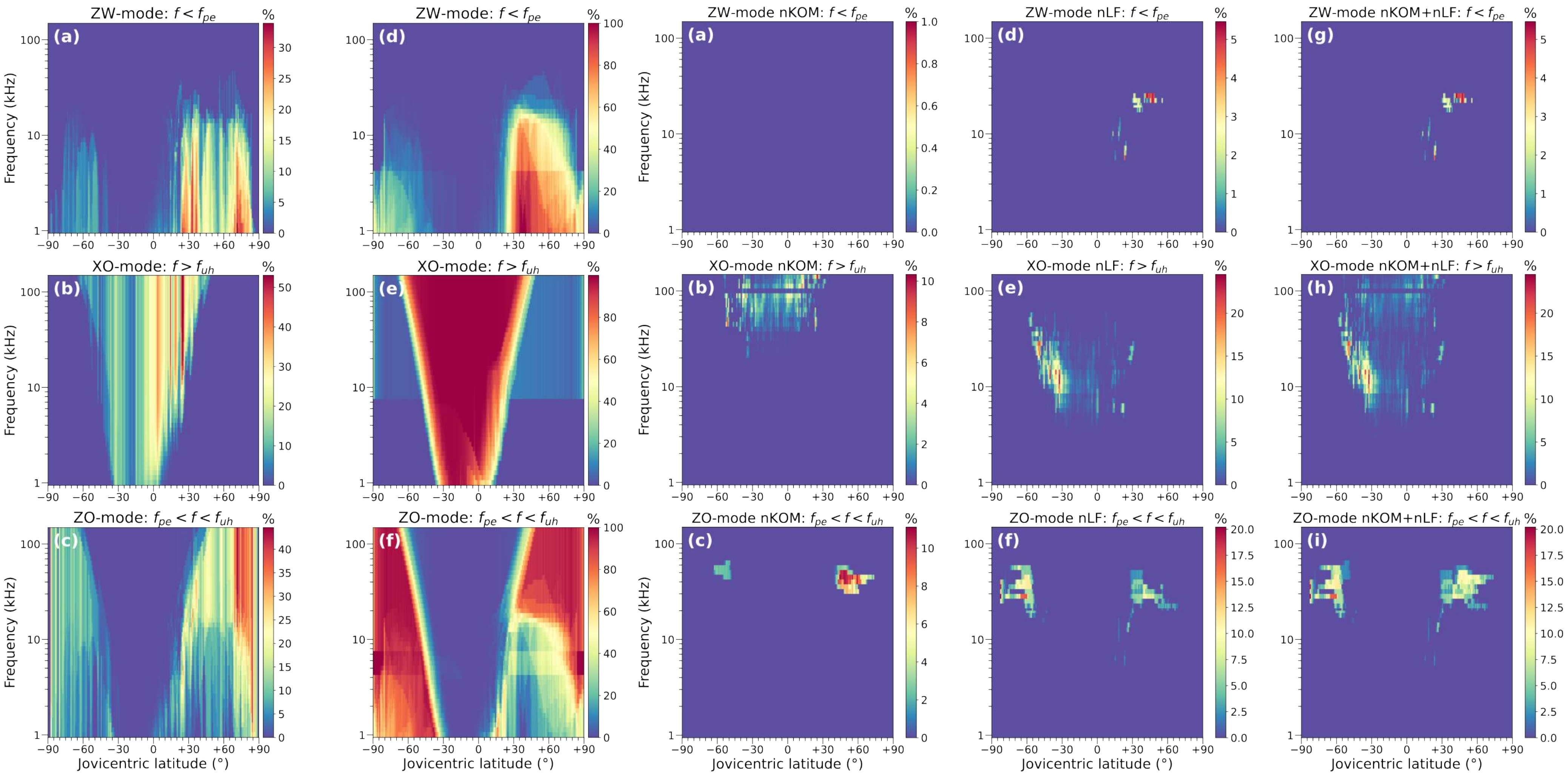

Initialisation : Simulation des observations de Juno

- Environnement :
  - Plasma : modèle de densité diffusif de Imai (2016) limité entre $4 - 13\ R_j$.
  - Champ magnétique : modèle de champ magnétique VIP4 de Connerney et al. (1998)
  - Maille du domaine de simulation : $0.1\ R_j$
- Observateur :
  - Trajectoire de Juno entre 2016 et 2019
  - Echantillonnage spatial suivant $\delta\theta = 1.5°$ et $\delta\phi = 2°$, en latitude et longitude.

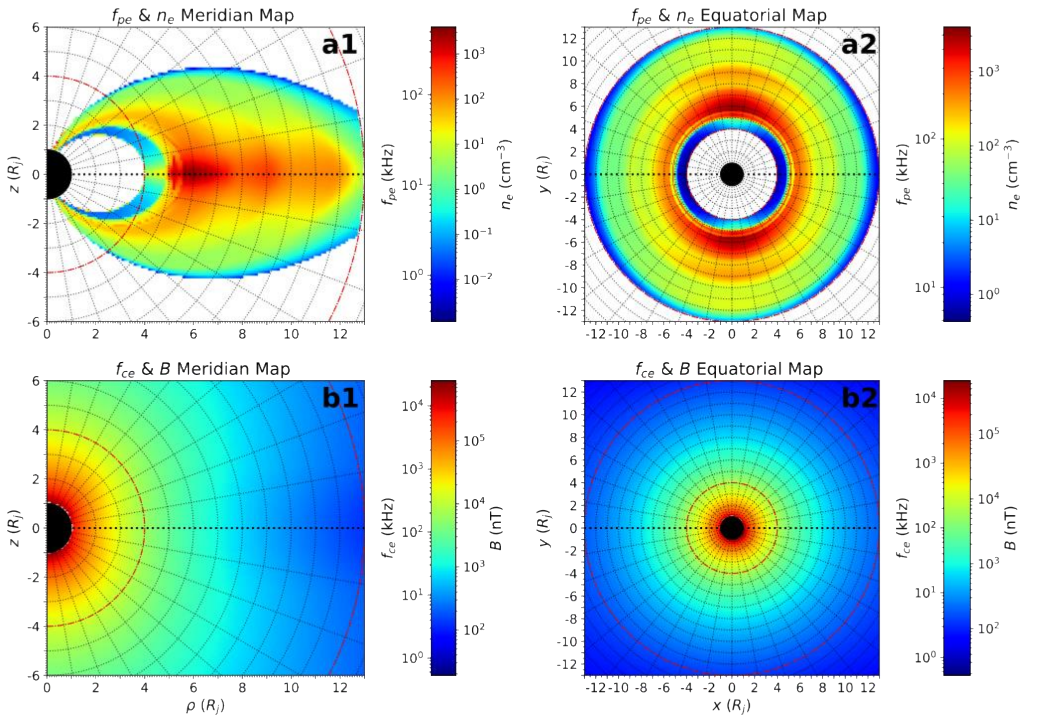

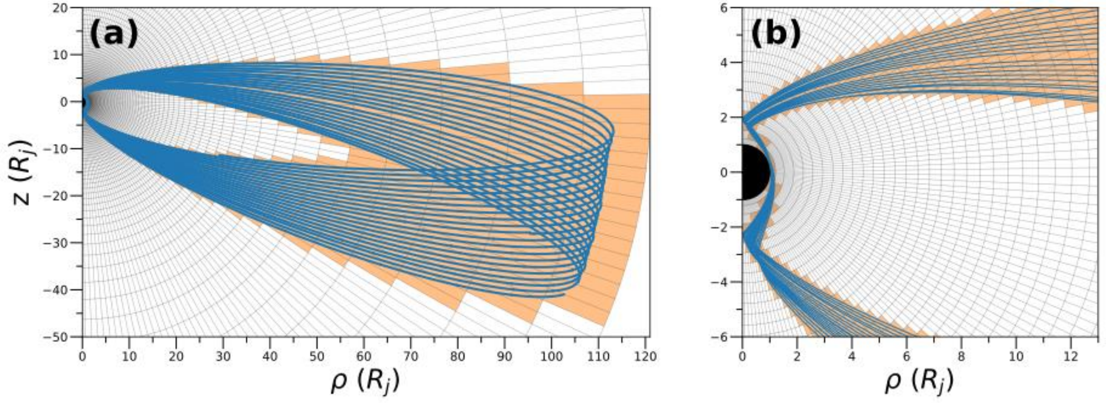

Plasma environment modeling

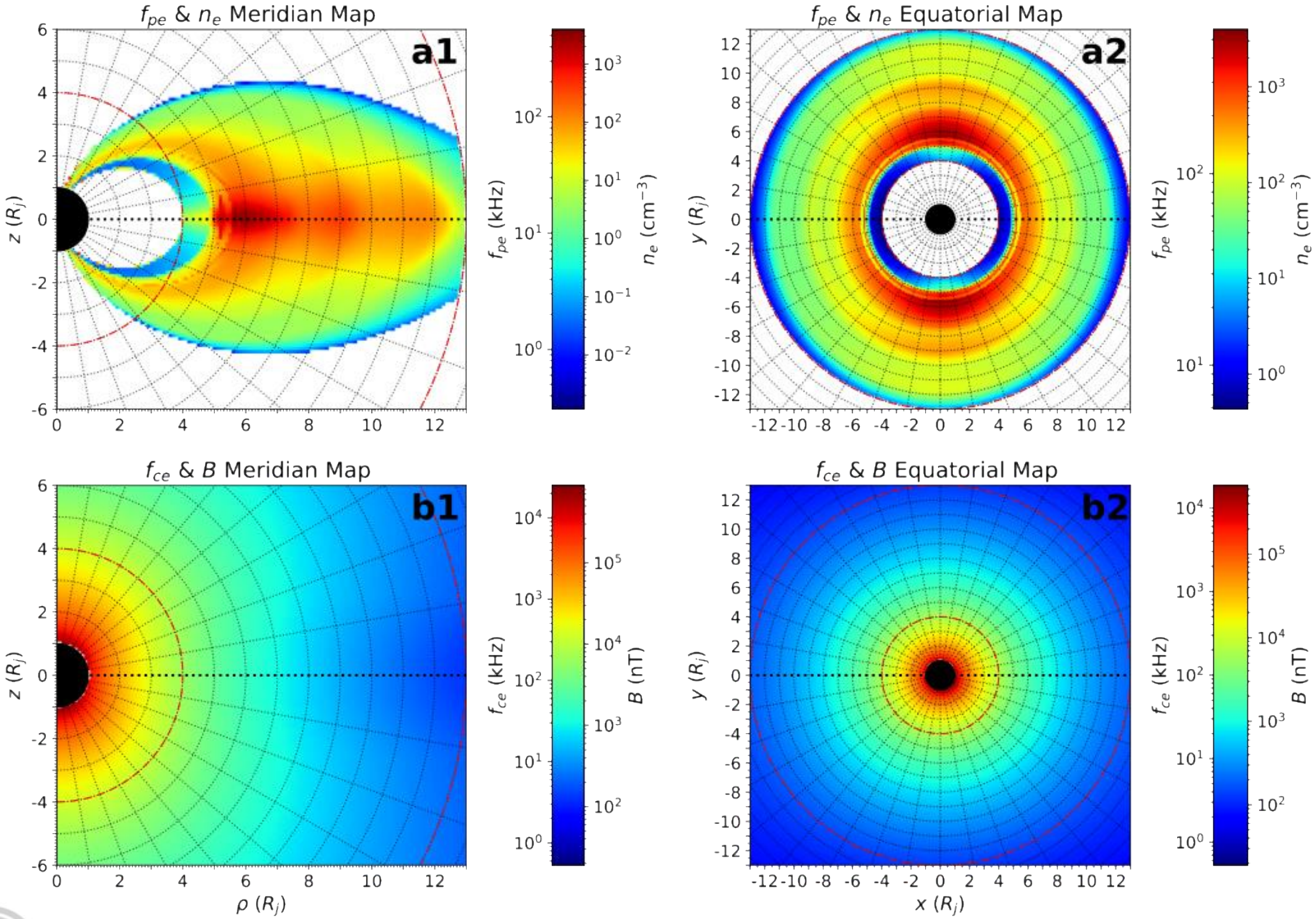

Cartes méridiennes et équatoriales de n_e et B prédites à partir des modèles de densité diffusif de Imai (2016) et de champ magnétique et disque de courant VIP4 (Connerney et al., 1998)

Sources activation parameters

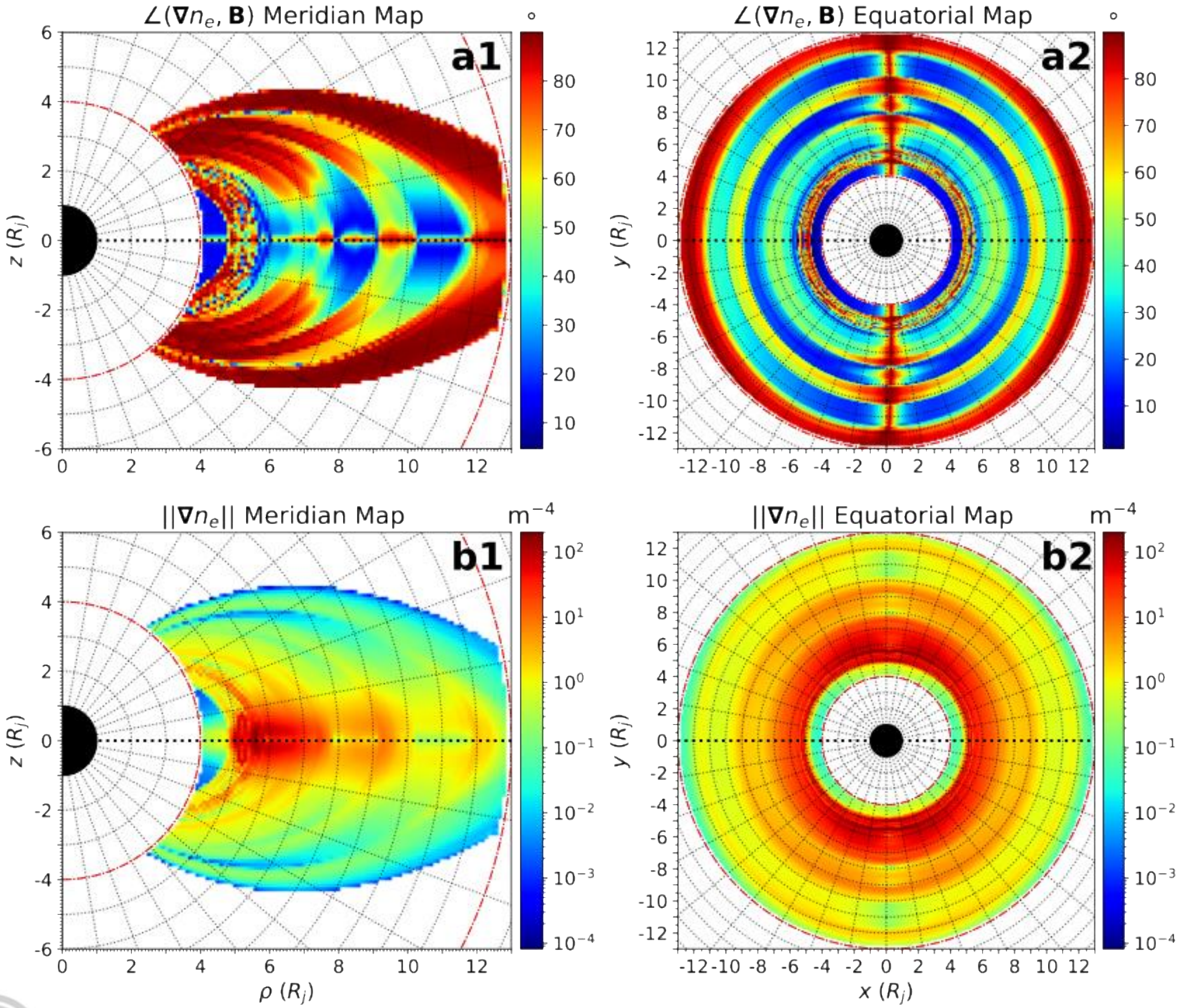

Cartes méridiennes et équatoriales de $\angle(\nabla n_e, B)$ et $||\nabla n_e||$ prédites à partir des modèles de densité diffusif de Imai (2016) et de champ magnétique et disque de courant VIP4 (Connerney et al., 1998)

ÚSTAV FYZIKY ATMOSFÉRY AV ČR, v. v. i. LIRA Observatoire de Paris | PSL

Distribution en fréquence de la norme du gradient

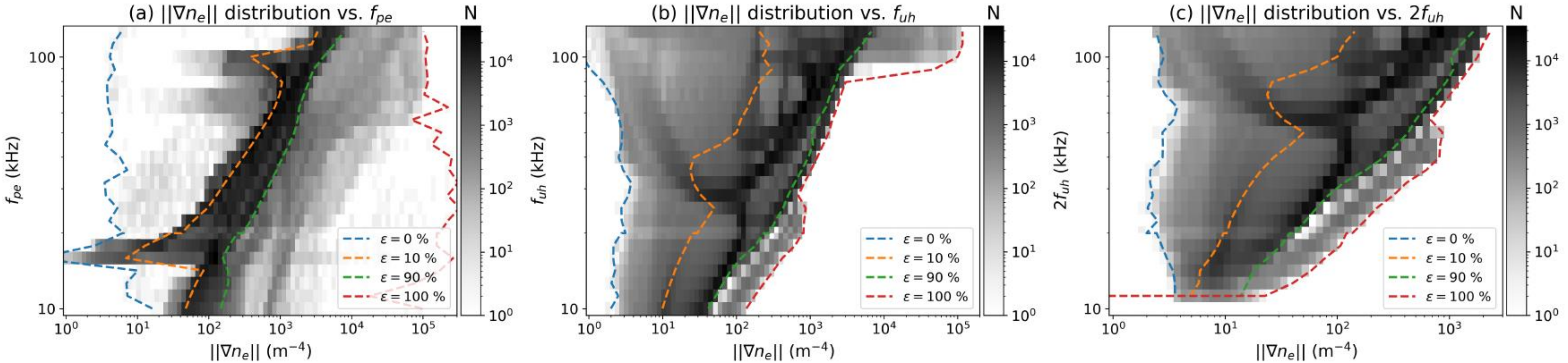

Correlation-inclusion coefficient

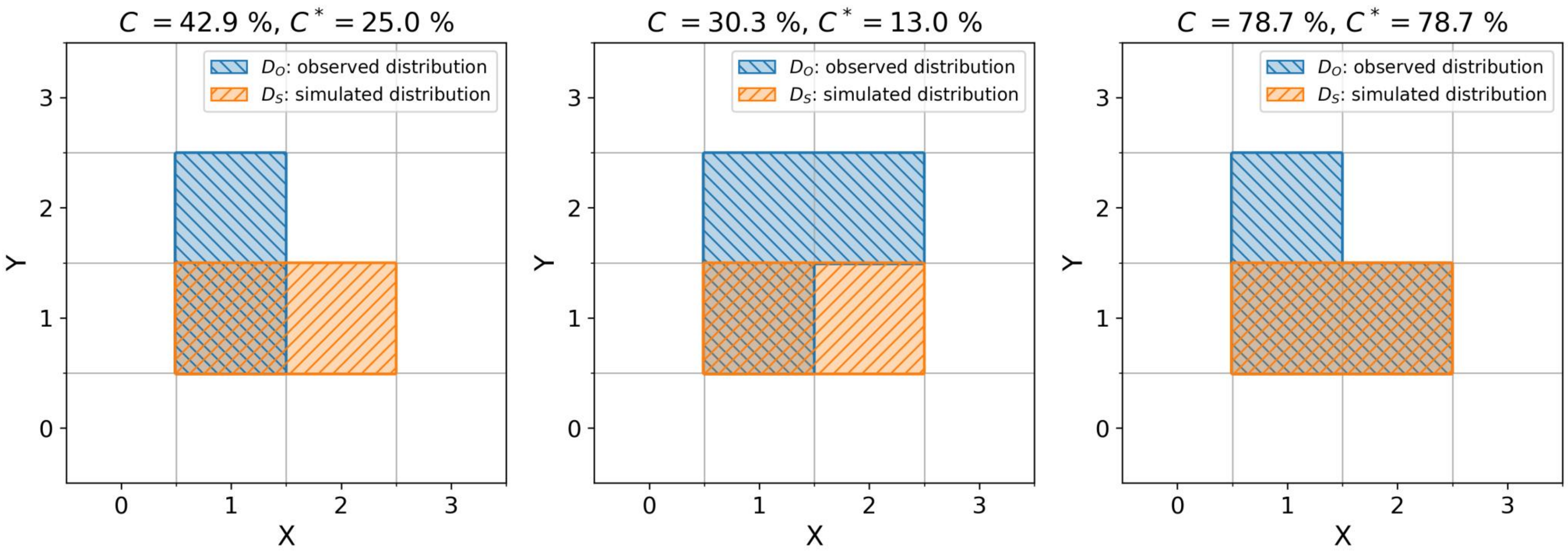

ÚSTAV FYZIKY ATMOSFÉRY AV ČR, v. v. i. LIRA Observatoire de Paris | PSL

Parametric study : generation scenario compatibility with the observations

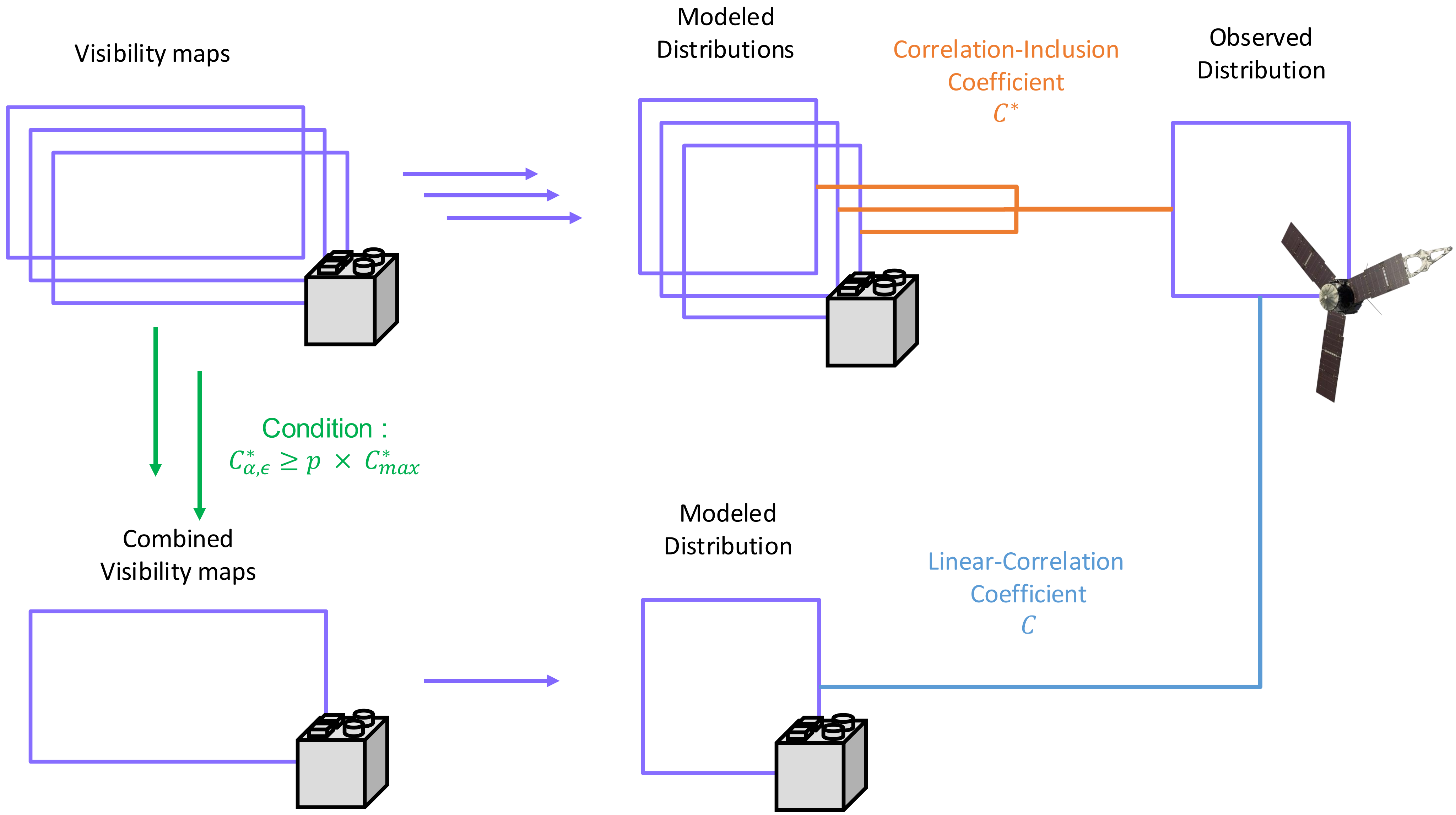

Exemple nKOM : compatibilité des scénarios de génération avec les observations

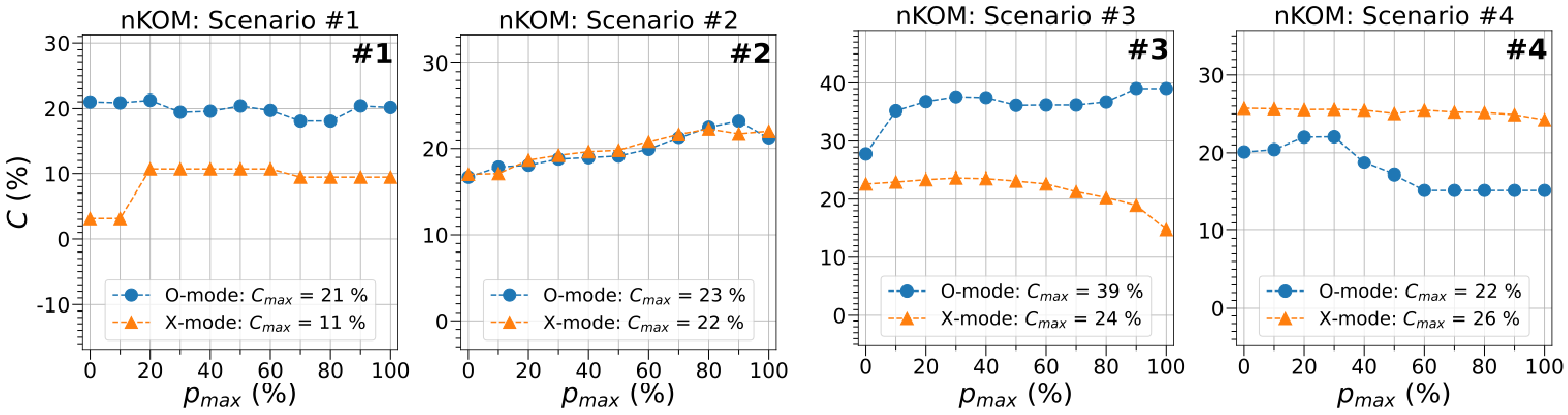

Exemple nKOM : compatibilité des scénarios de génération avec les observations

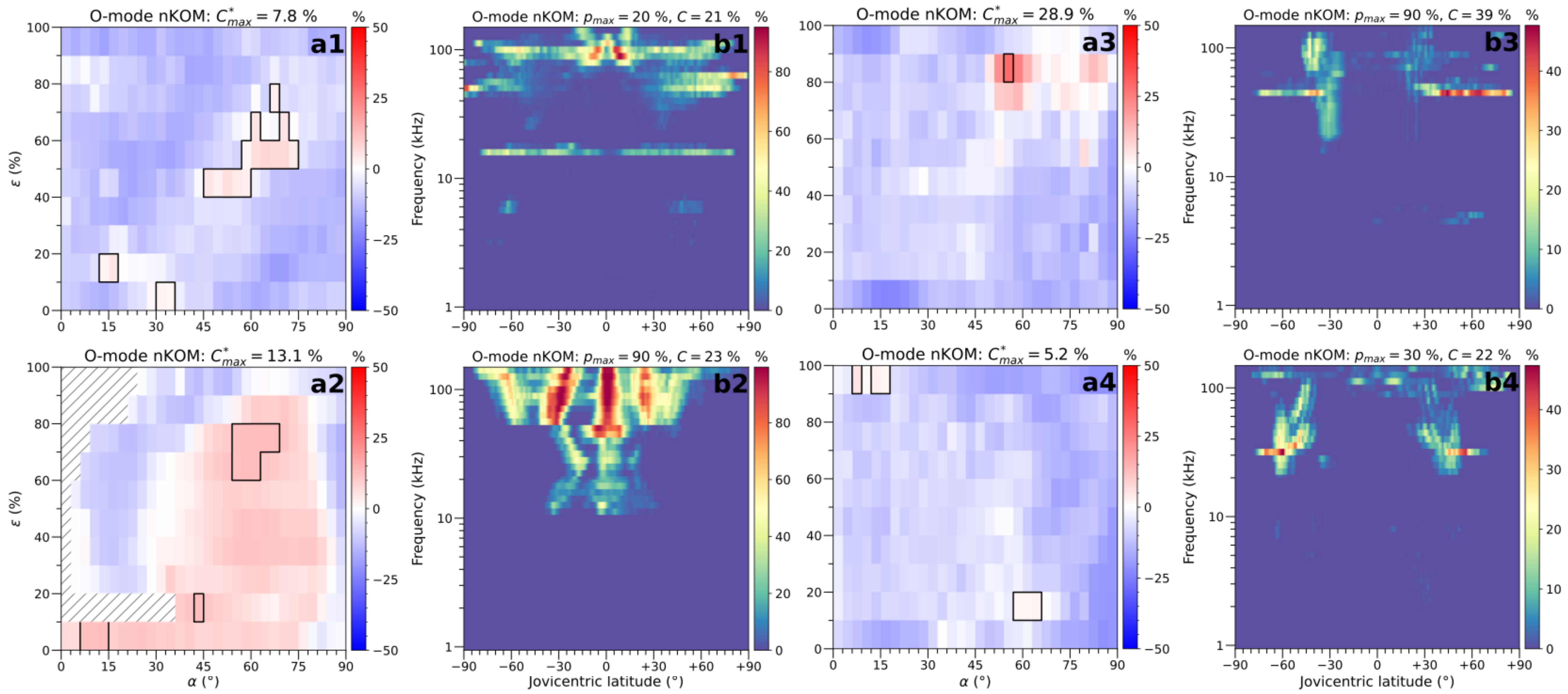

ÚSTAV FYZIKY ATMOSFÉRY
AV ČR, v. v. i.
LIRA
Observatoire de Paris
PSL

Mode XO : distribution du coefficient de corrélation-inclusion dans l'espace des paramètres (mode O)

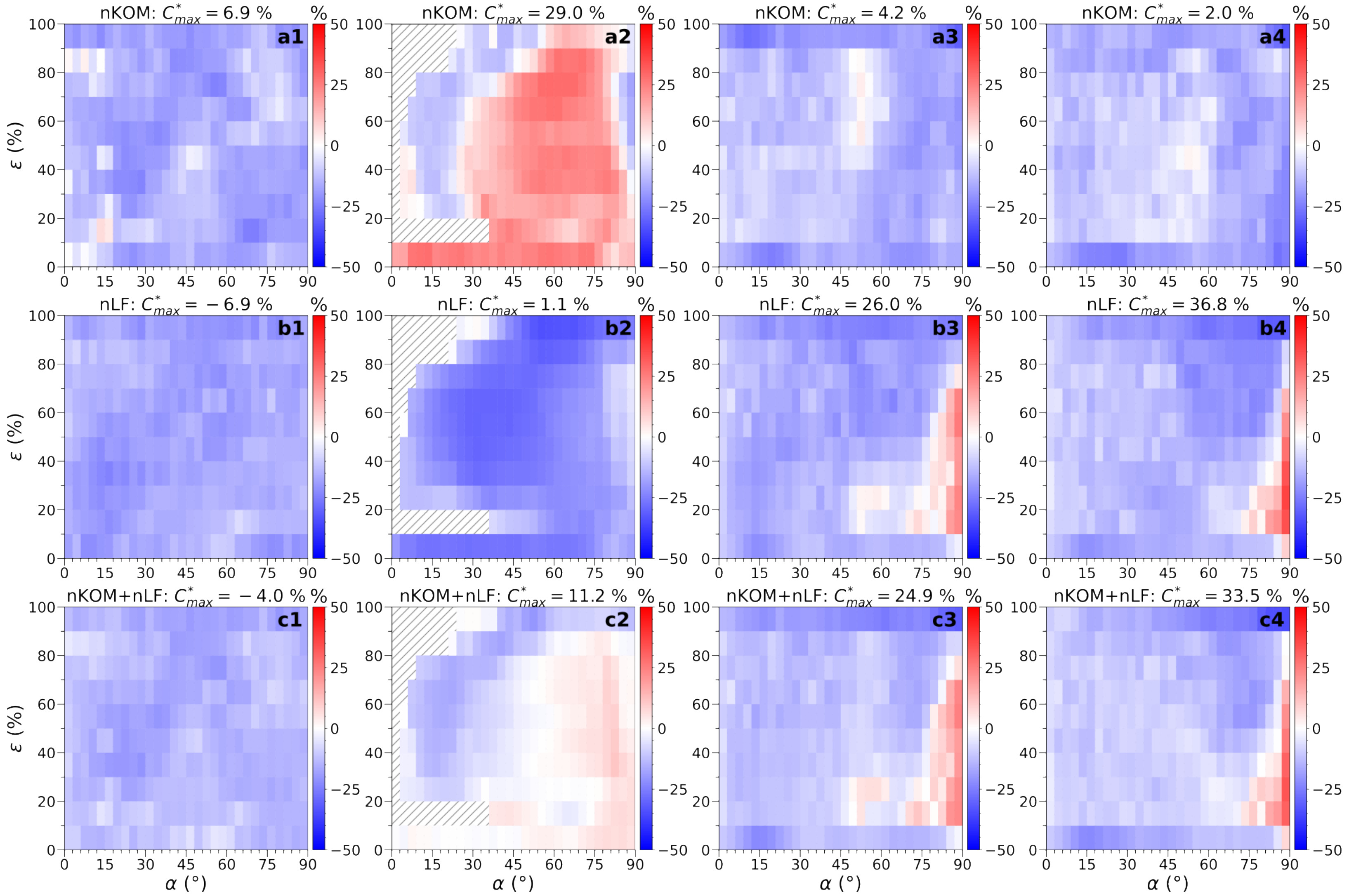

ÚSTAV FYZIKY ATMOSFÉRY AV ČR, v. v. i.
LIRA Observatoire de Paris | PSL

Mode XO : distribution du coefficient de corrélation-inclusion dans l'espace des paramètres (mode X)

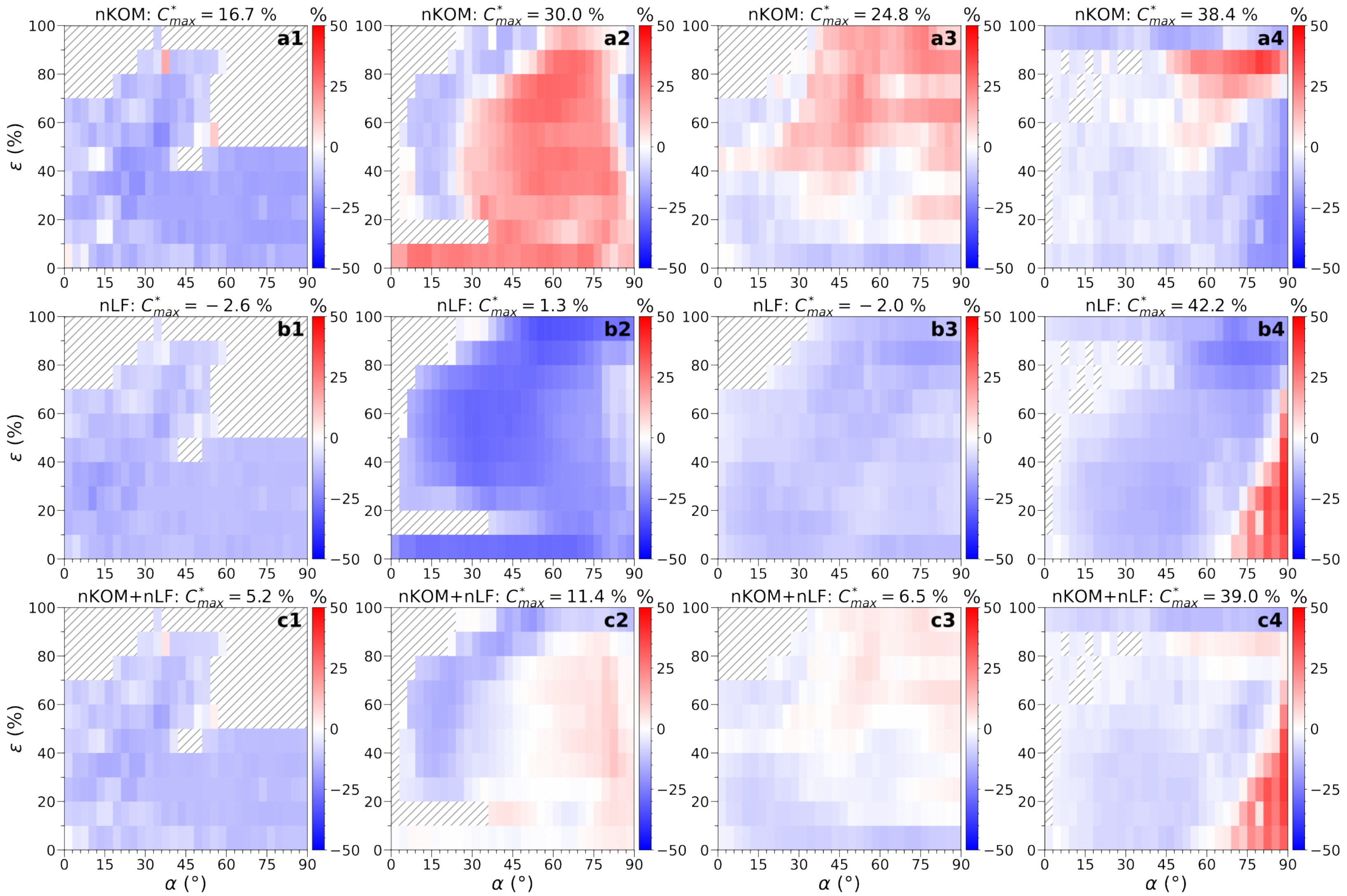

ÚSTAV FYZIKY ATMOSFÉRY AV ČR, v. v. i. | LIRA | Observatoire de Paris | PSL

Mode ZO : distribution du coefficient de corrélation-inclusion dans l'espace des paramètres (mode O)

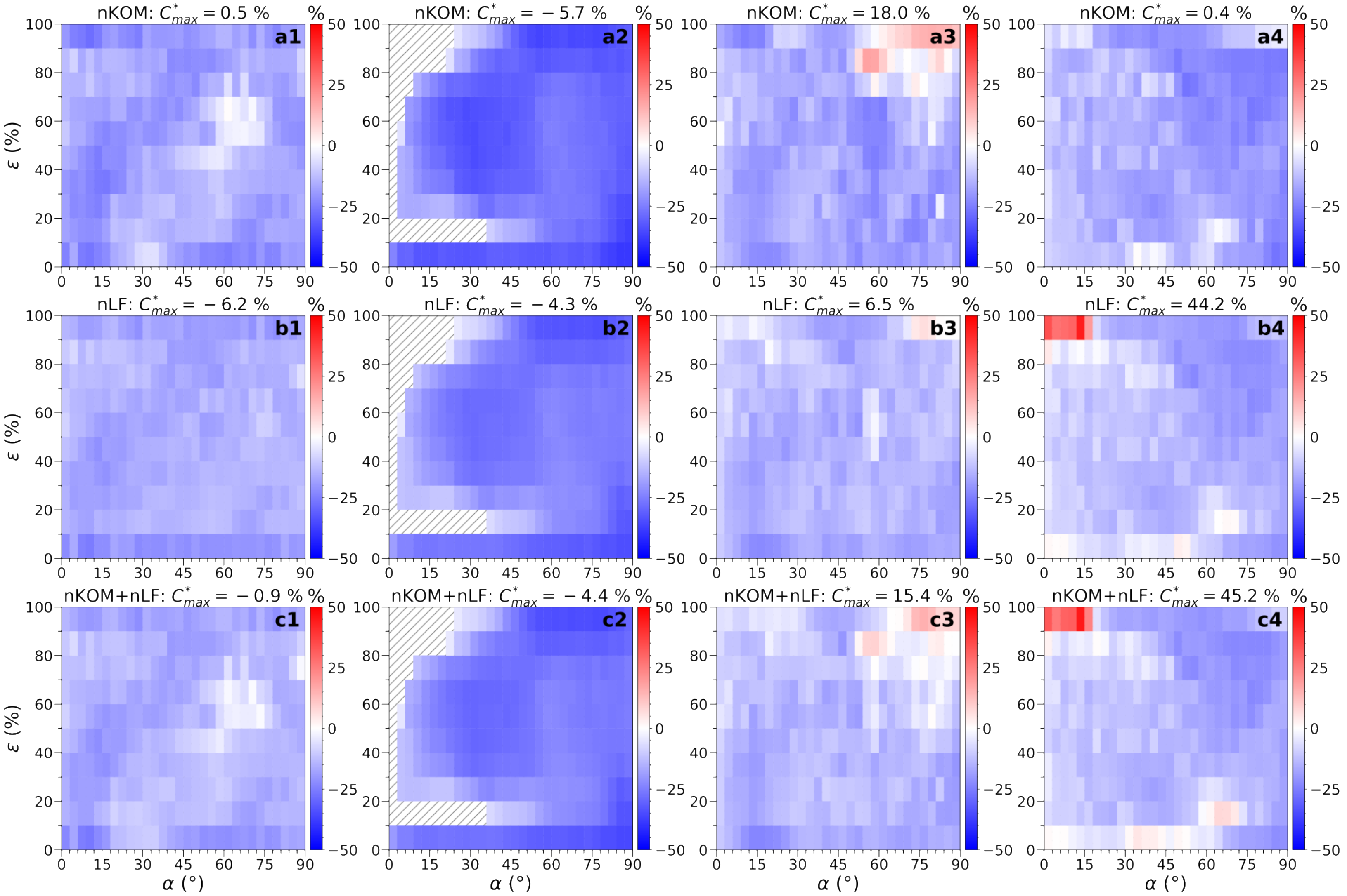

ÚSTAV FYZIKY ATMOSFÉRY AV ČR, v. v. i. LIRA Observatoire de Paris | PSL

Mode ZO : distribution du coefficient de corrélation-inclusion dans l'espace des paramètres (mode X)

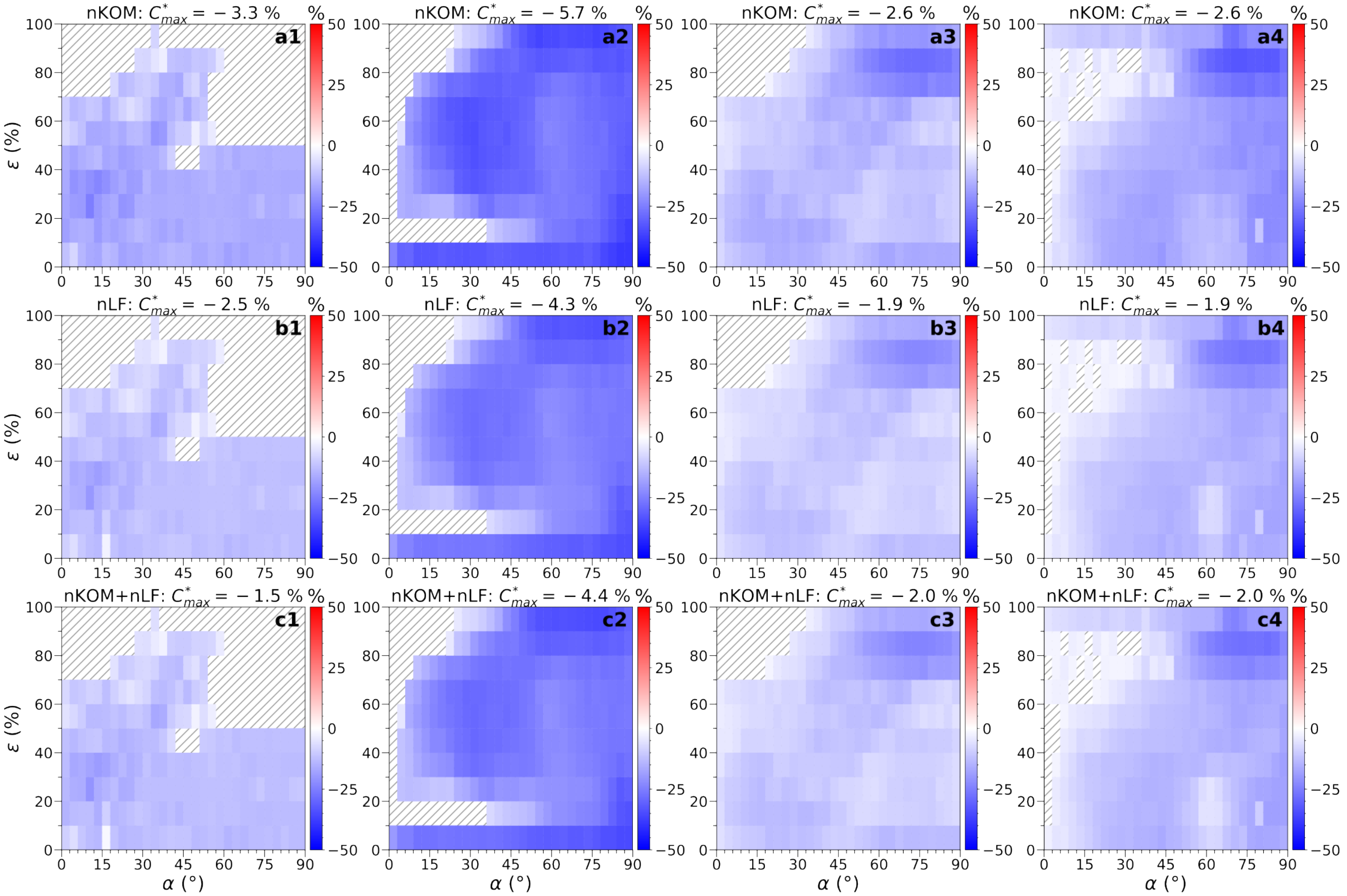

ÚSTAV FYZIKY ATMOSFÉRY AV ČR, v. v. i. LIRA Observatoire de Paris | PSL

Results: compatibility of the generation scenarios with all Juno-Waves observations

Coupure	Scénario	Corrélation Maximale C_{max}								
		nKOM			nLF			nKOM+nLF		
		Total	XO	ZO	Total	XO	ZO	Total	XO	ZO
mode O	#1	21%	26%	22%	-2%	5%	9%	8%	1%	12%
	#2	23%	**51%**	0%	1%	2%	-1%	13%	24%	-1%
	#3	**39%**	27%	**37%**	**41%**	**48%**	22%	**44%**	**46%**	29%
	#4	22%	25%	20%	**41%**	**45%**	**55%**	**45%**	**41%**	**54%**
mode X	#1	11%	20%	0%	-1%	0%	9%	4%	6%	9%
	#2	22%	**50%**	0%	1%	2%	-1%	12%	21%	-1%
	#3	24%	**47%**	0%	0%	0%	0%	7%	13%	0%
	#4	26%	**53%**	0%	**38%**	**49%**	0%	33%	**46%**	0%

LsPRESSO : Comparison with the nLF observations of the PJ01

- Imai et al. (2017) : nKOM and nLF sources locations for the Juno-Waves observations near the flyby of the PJ01.

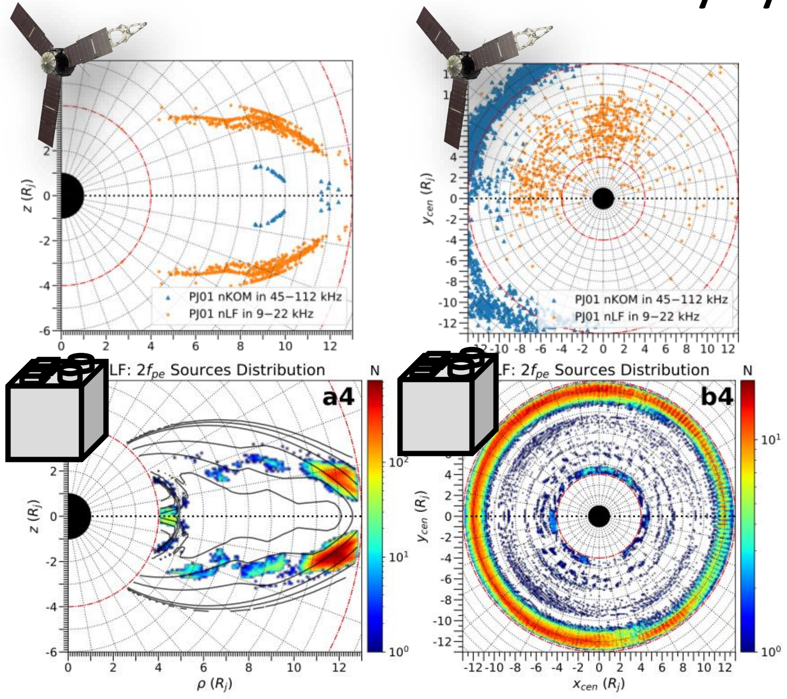

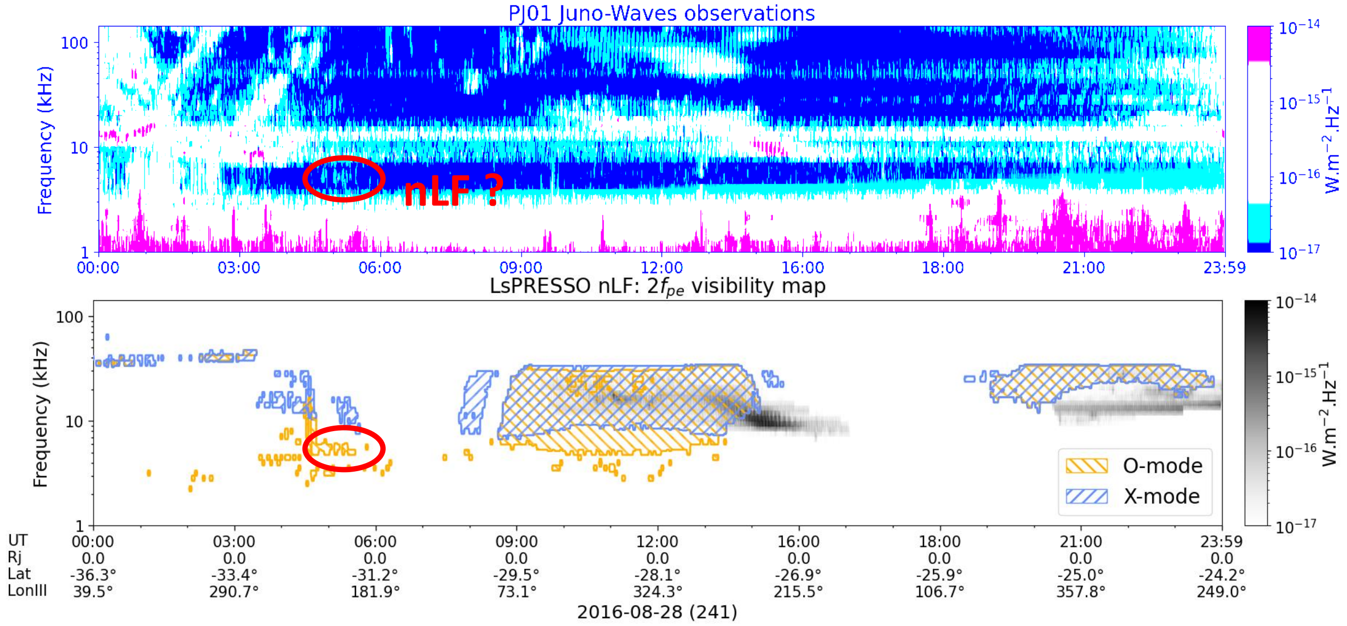

LsPRESSO: Comparison with the nKOM observations of the PJ01

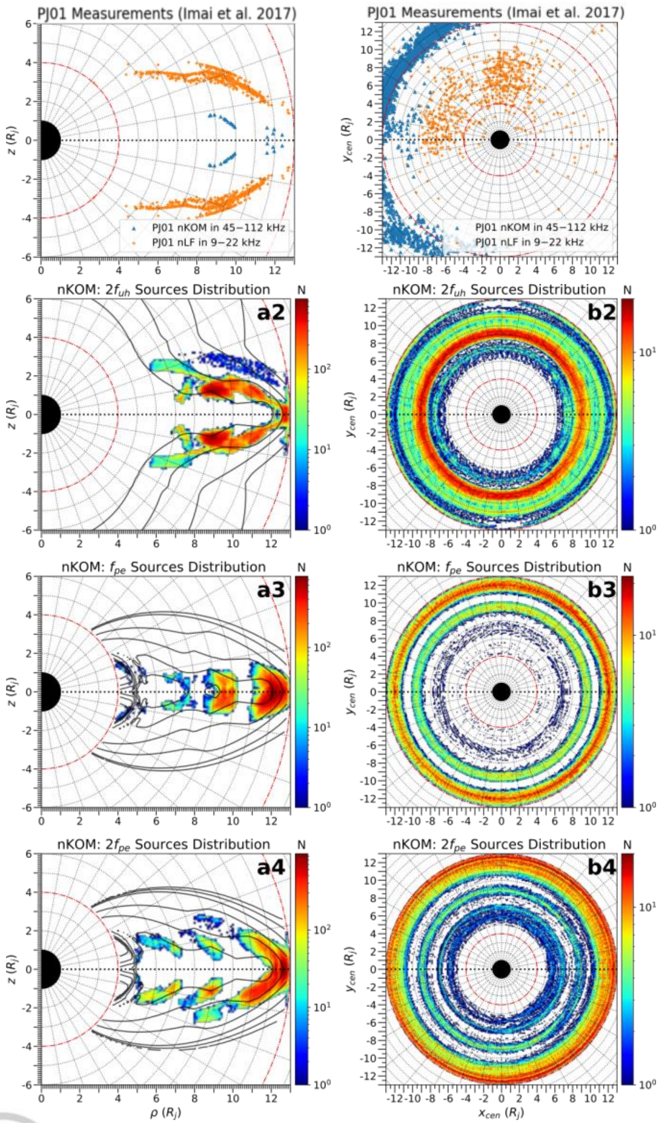

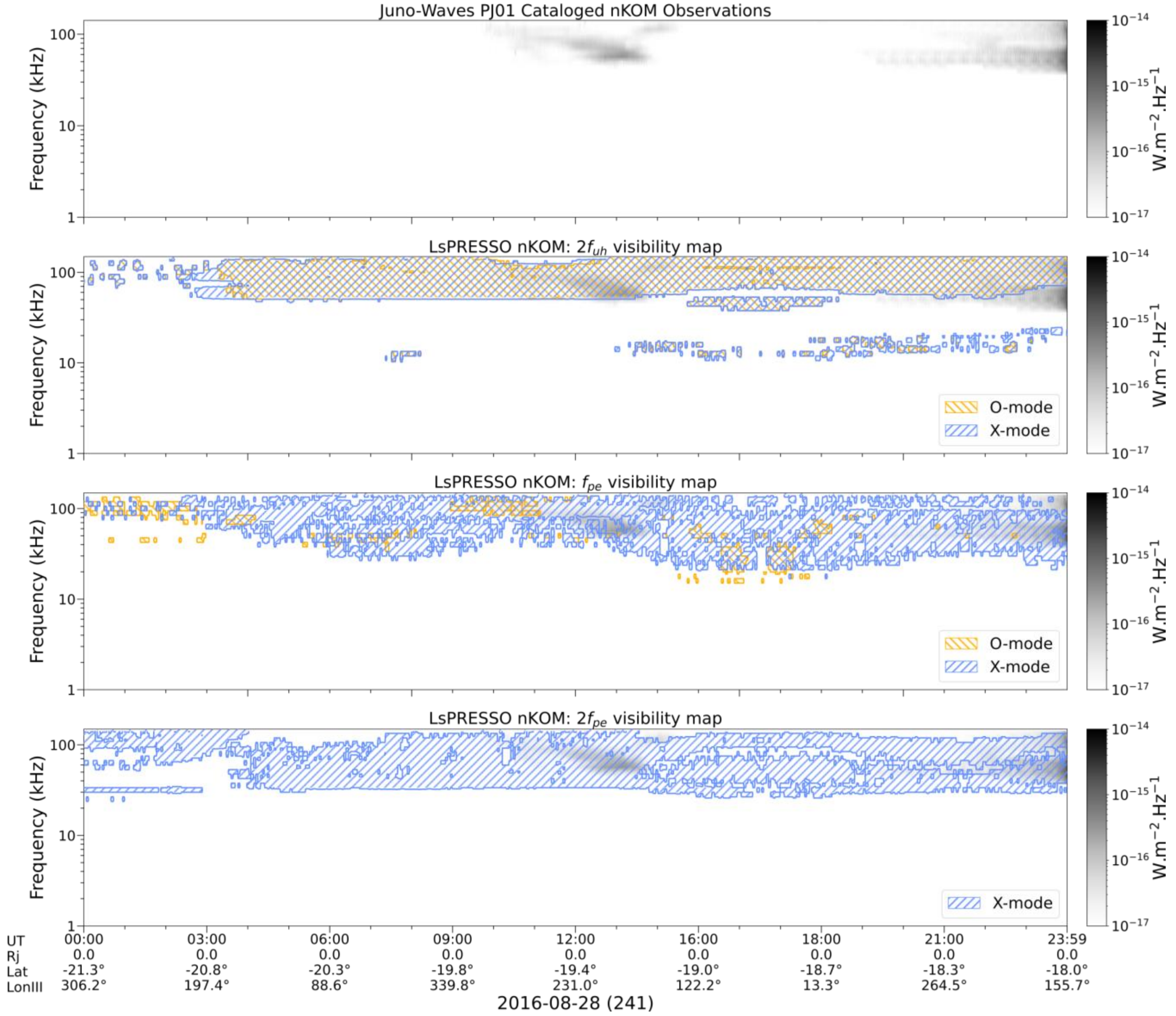

ÚSTAV FYZIKY ATMOSFÉRY AV ČR, v. v. i. LIRA Observatoire de Paris | PSL